Wireless Netw (2009) 15:365–389
DOI 10.1007/s11276-007-0055-4

A unified mobility model for analysis and simulation of mobile wireless networks

Ming Zhao · Wenye Wang

Published online: 15 September 2007

Abstract We propose a novel mobility model, named *Semi-Markov Smooth* (SMS) model, to characterize the smooth movement of mobile users in accordance with the physical law of motion in order to eliminate sharp turns, abrupt speed change and sudden stops exhibited by existing models. We formulate the smooth mobility model by a semi-Markov process to analyze the steady state properties of this model because the transition time between consecutive phases (states) has a discrete uniform distribution, instead of an exponential distribution. Through stochastic analysis, we prove that this model *unifies* many good features for analysis and simulations of mobile networks. First, it is smooth and steady because there is no speed decay problem for arbitrary starting speed, while maintaining uniform spatial node distribution regardless of node placement. Second, it can be easily and flexibly applied for simulating node mobility in wireless networks. It can also adapt to different network environments such as group mobility and geographic constraints. To demonstrate the impact of this model, we evaluate the effect of this model on distribution of relative speed, link lifetime between neighboring nodes, and average node degree by ns-2 simulations.

Keywords Mobility model · Smooth movement · Semi-Markov process · Stochastic analysis · Network performance evaluation · Mobile wireless networks

This work was supported by National Science Foundation under award CNS-0546289.

M. Zhao · W. Wang (✉)
Department of Electrical and Computer Engineering,
North Carolina State University, Raleigh, NC 27695, USA
e-mail: wwang@eos.ncsu.edu

1 Introduction

Mobility models are widely used in simulation studies for large-scale wireless networks, especially in the mobility-related research areas, such as routing protocol design [1], link and path duration analysis [2], location and resource management [3–5], topology control [6–8], and network connectivity issues [9–11] in cellular systems, wireless local area networks, and mobile ad hoc networks. There are many mobility models which have been well studied in survey papers [12, 13] which are focused on synthetic models, except few experimental studies [14, 15]. The challenge in designing mobility models is the trade-off between model efficiency and accuracy.

Due to easy analysis and simple implementation, *random mobility* models, in which each mobile node moves without constraint on its velocity, time period and destination, are most widely used [12]. For example, *random walk* (*RW*) model was originally proposed to emulate the unpredictable movements of particles in physics, also known as Brownian motion [12]. Compared to the RW model, *Random Waypoint* (*RWP*) model [16] is often used to evaluate the performance of mobile ad hoc networks (MANETs) due to its simplicity. However, two flaws have been found in its stationary behavior. First, Yoon showed that the average node speed of RWP model decreases over time [17]. Second, Bettstetter [18] and Blough et al. [19] respectively observed that RWP model has non-uniform spatial node distribution at steady state, with the maximum node density in the middle of simulation region given that initial state is uniform distribution. This implies that analysis and simulations based on RWP model may generate misleading results. To overcome the non-uniform spatial node distribution problem in RWP model, Nain and Towsley recently showed that

random direction (*RD*) model [20] with warp or reflection on the border has uniformly distributed user position and direction in [21]. Recently, Boudec et al. proposed a generic random mobility model, called *Random Trip* (*RT*) model, which covers RW, RWP and RD models, as well as their variants [22].

Random mobility models describe the mobility pattern in a *macroscopic level*, that is, mobile nodes do not change speed or direction within one movement. Thus, random mobility models can fit vehicular and large-scale environments. Therefore, they are insufficient to mimic the minute moving behaviors of mobile users, such as speed acceleration and smooth direction changes within one movement. The movements presented by random models are completely uncorrelated or random, thus demonstrating unrealistic moving behaviors, such as sudden stop, sudden acceleration, and sharp turn frequently occur during the simulation [12]. These abrupt speed and direction change events will influence the network topology change rate, which further significantly affect network performance. In consequence, the simulation results and theoretical derivations based on random mobility models may not correctly indicate the network performance and effects of system parameters.

As an effort to resolve the problem of unrealistic movements and to provide smooth behaviors, mobility models that consider the correlation of node's moving behavior are proposed, which are called *temporal* models [12], such as *Smooth Random* (*SR*) model [23] and *Gauss–Markov* (*GM*) model [24]. SR model considers the smooth speed and direction transitions for mobile nodes. In the SR model, a node moves at a constant speed along a specific direction until either a speed or direction change event occurs according to independent Poisson process. In the GM model, the velocity of a mobile node at any time slot is a function of its previous velocity with a Gaussian random variable. Although both SR and GM models can be used for either cellular environments or ad hoc networks, they also have application limitations. In the SR model, because of the assumption of Poisson process, the uncertainty of the speed and direction change within each movement make it difficult to evaluate network performance according to a specific node mobility requirement. Moreover, an SR movement may have new speed change during the speed transition and does not stop unless a targeting speed is specified as zero, which is not flexible for movement control. In the GM model, mobile nodes cannot travel along a straight line [13] as long as the temporal correlation (memorial) parameter is not equal to 1, and they do not stop during the simulation. However, in reality, vehicles usually move along a straight line for a period of time and mobile users always move in an intermittent way with a random pause time.

Therefore, we are motivated to design a new mobility model that can abide by the physical law of moving objects to avoid abrupt moving behaviors, and can provide a *microscopic view* of mobility such that node mobility is controllable and adaptive to different network environments.[1] In summary, this model is expected to *unify* the desired features as follows:

1. *Smooth and sound movements*: A mobility model should have temporal features, i.e., a mobile node's current velocity is dependent on its moving history so that smooth movements can be provided and mobile nodes should move at stable speed without the average speed decay problem [25].
2. *Consistency with the physical law of a smooth motion*: In order to mimic the kinetic correlation between consecutive velocities in a microscopic level, a mobility model should be consistent with the physical law of a smooth motion in which there exists acceleration to start, stable motion and deceleration to stop for controllable mobility [26, 27].
3. *Uniform nodal distribution*: As most of analytical studies of MANETs are based on the assumption of uniform nodal distribution, such as network capacity and delay [28], network connectivity, topology control [10] and link change rate [29], a mobility model should be able to generate uniform spatial node distribution at steady-state. Otherwise, the non-uniform node distribution caused by a mobility model may invoke misleading information and results [21].
4. *Adaptation to diverse network application scenarios*: In order to properly support rich MANET applications having complex node mobility and network environments, such as group mobility and geographic restriction, a generic mobility model which is adaptive to different mobility patterns is highly desirable.

The contributions of this paper include theoretical modeling of smooth movement, steady-state analysis, and simulation studies of the impacts of the proposed mobility model. First, we propose a *unified*, *smooth* model, namely *Semi-Markov Smooth* (SMS) model, which includes four consecutive phases: *Speed Up* phase, *Middle Smooth* phase, *Slow Down* phase, and *Pause* phase, based on the physical law of a smooth motion. Second, our proposed SMS model is a *unified* mobility model, which can model *the mobility patterns of users at varying levels of granularity*, i.e., both the macroscopic level and the microscopic level. Third, we prove that the proposed SMS model is smooth, which eliminates sharp turns and sudden stops; it is steady because there is no speed decay problem for arbitrary

[1] An earlier version appeared in the proceeding of IEEE GLOBECOM 2006 [24].

starting speed and it maintains uniform spatial node distribution during the entire simulation period. These nice properties are also verified by ns-2 simulations. Besides, we demonstrate the implementation of the proposed model to serve diverse application scenarios, such as group mobility and geographic restrictions. Finally, we present multiple impacts of the SMS model on MANETs: the relative speed between a pair of mobile nodes, which shows a Rayleigh distribution; the CDF of link lifetime and average node degree, which demonstrate that network connectivity evaluation based on the RWP model in current simulation tool such as ns-2 is over optimistic.

Tabel 1 illustrates a detail comparison based on properties of current typical mobility models and those of our proposed SMS model, where independent mobility parameters: *speed* (V), *movement duration* (T), *destination* (D) and *direction* (θ) with respect to different mobility patterns are also included.

The remainder of the paper is organized as follows. Section 2 describes the mobility pattern and stochastic process of the proposed SMS model. Section 3 analyzes the stochastic properties of SMS movement, including probability distribution and expected value of movement duration, speed, and trace length. Section 4 proves that steady-state speed exists and there is no average speed decay in the SMS model. Section 5 validates the analysis of SMS properties with simulations. Section 6 shows that the SMS model can be easily implemented for different mobility scenarios such as group mobility and geographic constraints, followed by the effects of the SMS model on network architecture. Finally, the paper is concluded in Sect. 7.

2 A unified mobility model: SMS model

In this section, we present a novel mobility model, SMS model with detailed mobility patterns. Specifically, within one movement, we elaborate when and how an SMS node changes its speed and direction; how the node accelerates and decelerates the speed; and how strong the temporal correlation is during the speed and direction change. By answering these questions, the moving behaviors of mobile nodes can be deeply understood and well manifested by the proposed model. Further, we describe the stochastic process of the SMS model. We consider it as a *renewal process* with respect to consecutive SMS movements and regard it as a *semi-Markov* process in the study of iterative phases transition.

2.1 Model description

According to the fundamental physical law of a smooth motion, a moving object would experience *speed acceleration*, *stable speed*, and *speed deceleration* during a movement. This implies that a smooth movement should contain multiple moving stages, and a temporal correlation exists during the speed transition. Therefore, based on the physical law of smooth motion, our proposed SMS model consists of four consecutive phases: *Speed Up* phase, *Middle Smooth phase*, *Slow Down* phase, and *Pause* phase. Throughout this paper, we define one SMS *movement* or *movement duration* as the time period that a node travels from the starting point to its next position that the node stops moving. Each movement is quantized into $\mathcal{K}$ equidistant time steps, where $\mathcal{K} \in \mathbb{Z}$. The time interval between two consecutive time steps is denoted as Δt (s). The SMS model is an entity model which determines the mobility pattern of each user individually, which is designed with the following assumptions:

- All mobile nodes move independently from others and have the identical stochastic properties.
- For any mobile nodes, every SMS movement has identical stochastic properties.
- Within each SMS movement, a mobile node's velocity at current time step is dependent on its moving history.

Here, the first two assumptions are similar to the random mobility models for better supporting theoretical studies as well system performance evaluation of MANETs. To be

Table 1 Properties of different mobility models

Attributes	RW [30]	RWP [16]	RD [21]	SR [23]	GM [24]	SMS
Parameters	V, θ	V, D	V, θ, T	V, θ	V, θ	V, θ, T
Movement phases	{moving, pause}	{moving, pause}	{moving, pause}	{moving, pause}	{moving}	{speed-up, middle smooth, slow-down, pause}
Smoothness	No	No	No	Yes	Yes	Yes
Speed decay	May	Yes	No	No	No	No
Uniform node distribution	Close	No	Yes	Close	Yes	Yes
Mobility scale	Macroscopic	Macroscopic	Macroscopic	Microscopic	Microscopic	Microscopic
Unified model	No	No	No	No	No	Yes
Controllability	Low	Low	Low	Medium	Medium	High

distinguished from random mobility models, the third assumption of the SMS model is especially used for describing microscopic smooth nodal movements. Next, we describe the SMS model based on the single user mobility. The implementation for group mobility and geographic constraints will be explained in Sect. 6.

2.1.1 Speed up phase (α-phase)

For every movement, an object needs to accelerate its speed before reaching a stable speed. In this phase, the movement pattern of an SMS node is exploited from what is defined in SR model [23]. Thus, the first phase of a movement is called *Speed up* α-phase, which covers the time interval $[t_0, t_\alpha] = [t_0, t_0 + \alpha\Delta t]$. At initial time t_0 of a movement, the node randomly selects a *target speed* $v_\alpha \in [v_{\min}, v_{\max}]$, a *target direction* $\phi_\alpha \in [0, 2\pi]$, and the total number of *time steps* α for the speed up phase. $\alpha \in \mathbb{Z}$ and is selected in the range of $[\alpha_{min}, \alpha_{\max}]$. These three random variables are independently uniformly distributed. Note that $\alpha_{\min}$ and $\alpha_{\max}$ imply the physical speed-up capabilities of the node. For instance, when α is selected close to $\alpha_{\max}$, the transition time is long, but the degree of temporal correlation is strong.

In reality, an object typically accelerates the speed along a straight line. Thus, the direction ϕ_α does not change during this phase. To avoid sudden speed change, the node will evenly accelerate its speed along direction ϕ_α from starting speed $v(t_0) = 0$, to the target speed v_α, which is the ending speed of α-phase, i.e., $v(t_\alpha) = v_\alpha$. Hence, the mobility pattern in speed up α-phase is represented by a triplet (α, v_α, ϕ_α). The acceleration rate at α-phase, a_α, can be obtained by

$$a_\alpha = \frac{v_\alpha - v(t_0)}{t_\alpha - t_0} = \frac{v_\alpha}{\alpha\Delta t}. \tag{1}$$

An example of speed change in α-phase is shown in Fig. 1(a), where the node speed increases evenly step by step and reaches the target speed v_α by the end of this phase.

2.1.2 Middle smooth phase (β-phase)

After the initial acceleration, a moving object will have a smooth movement, even though moving speed and direction may change. Accordingly, once the node transits into β-phase at time t_α, the node randomly selects β time steps and moves into β-phase. During time interval $(t_\alpha, t_\beta] = (t_\alpha, t_\alpha + \beta\Delta t]$, where $\beta \in \mathbb{Z}$ is uniformly distributed over $[\beta_{min}, \beta_{\max}]$. As a succeeding phase of α-phase, the initial value of speed v_0 and direction ϕ_0 in β-phase are v_α and ϕ_α, respectively. The speed and direction during β-phase then change on the basis of v_α and ϕ_α at a memory level parameter ζ, which ranges over [0, 1] and is constant for both speed and direction at each time step. Thus, by adjusting parameter ζ, we can easily control the degree of temporal correlation of velocity between two consecutive steps. For example, let us assume that the standard deviation σ_v and σ_ϕ are 1, which implies that the speed or direction difference between two consecutive time steps is less than 1 m/s or 1 rad within β-phase. Through simulations, we find that this granularity is sufficient to describe user mobility.

Then the step speed (i.e., speed at a time step) and step direction (i.e., direction at a time step) at the jth time step for an SMS node in β-phase are presented by:

$$\begin{aligned} v_j &= \zeta v_{j-1} + (1-\zeta)v_\alpha + \sqrt{1-\zeta^2}\,\widetilde{V}_{j-1} \\ &= \zeta^j v_0 + (1-\zeta^j)v_\alpha + \sqrt{1-\zeta^2}\sum_{m=0}^{j-1}\zeta^{j-m-1}\widetilde{V}_m \\ &= v_\alpha + \sqrt{1-\zeta^2}\sum_{m=0}^{j-1}\zeta^{j-m-1}\widetilde{V}_m, \end{aligned} \tag{2}$$

and

$$\begin{aligned} \phi_j &= \zeta\phi_{j-1} + (1-\zeta)\phi_\alpha + \sqrt{1-\zeta^2}\,\widetilde{\phi}_{j-1} \\ &= \phi_\alpha + \sqrt{1-\zeta^2}\sum_{m=0}^{j-1}\zeta^{j-m-1}\widetilde{\phi}_m, \end{aligned} \tag{3}$$

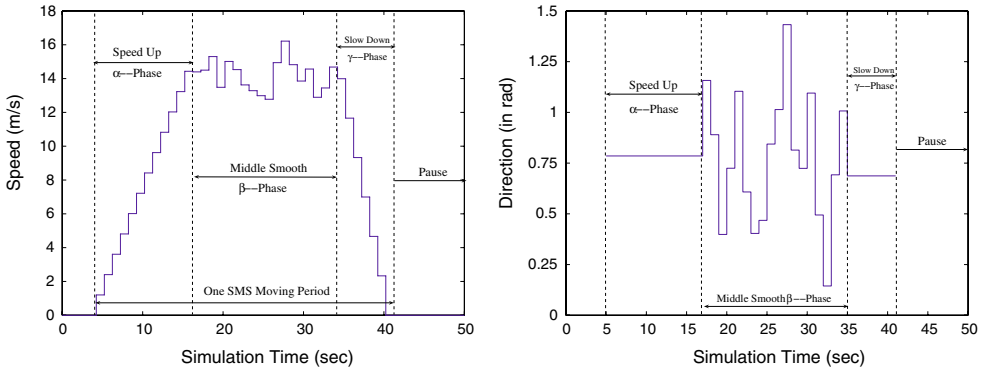

Fig. 1 An example of speed and direction transition in one SMS movement

(a) Speed vs. Time in One SMS Movement. **(b)** Direction vs. Time in One SMS Movement.

where $\widetilde{V}_j$ and $\widetilde{\phi}_j$ are two stationary Gaussian random variables with zero mean and unit variance, independent from V, and ϕ_j, respectively. By substituting β for j into (2) and (3), the ending step speed v_β and ending step direction ϕ_β of β-phase are obtained as:

$$\begin{aligned} v_\beta &= v_\alpha + \sqrt{1-\zeta^2}\sum_{m=0}^{\beta-1}\zeta^{\beta-m-1}\widetilde{V}_m, \\ \phi_\beta &= \phi_\alpha + \sqrt{1-\zeta^2}\sum_{m=0}^{\beta-1}\zeta^{\beta-m-1}\widetilde{\phi}_m. \end{aligned} \tag{4}$$

Given (2) and (3), the mobility pattern in β-phase is represented by a quartet (β, v_α, ϕ_α, ζ). As shown in Fig. 1(a), node speed fluctuates around the speed v_α achieved at the end of α-phase in each step of β-phase. In an SMS movement, β-phase is the main moving phase, which characterizes the mobility level and direction for a node during the entire movement.

2.1.3 Slow down phase (γ-phase)

According to the physical law of motion, every moving object needs to reduce its speed to zero before a full stop. In order to avoid the sudden stop event happening in the SMS model, we consider that the SMS node experiences a slow down phase to end one movement. In detail, once the node transits into γ-Phase, i.e., slow down phase, at time t_β, it randomly selects γ time steps and a direction ϕ_γ. Hence, γ-phase contains the last γ time steps of one SMS movement over time interval $(t_\beta, t_\gamma] = (t_\beta, t_\beta + \gamma\Delta t]$, where $\gamma \in \mathbb{Z}$ and is uniformly distributed over $[\gamma_{min}, \gamma_{\max}]$. The SMS node will evenly decelerate its speed from v_β to $v_\gamma = 0$. The rightmost part in Fig. 1(a) shows an example of speed change in γ-phase. In reality, a moving object typically decelerates the speed along a straight line before a full stop. Thus, the direction ϕ_γ does not change during the γ-phase. In order to avoid the sharp turn event happening during the phase transition, ϕ_γ and ϕ_β are correlated. Specifically, ϕ_γ is obtained from (3), by substituting β for $j-1$. At the end of γ-phase, i.e., t_γ, a mobile node stops at the destination position of its current movement. Thus, the mobility pattern in γ-phase is represented by a triplet (γ, v_β, ϕ_γ). The deceleration rate a_γ is given by:

$$a_\gamma = \frac{v_\gamma - v_\beta}{t_\gamma - t_\beta} = -\frac{v_\beta}{\gamma\Delta t}. \tag{5}$$

Figure 1(a) shows an example of speed vs. time during one SMS movement, which contains a total number of $\mathcal{K} = 37$ small consecutive steps, where α-phase contains 12 time steps, β-phase includes 18 time steps, and γ-phase consists of 7 time steps. After each movement, a mobile node may stay for a random pause time T_p. Correspondingly, Fig. 1(b) illustrates the node's direction behavior of the same SMS movement. It is clear to observe that the direction is constant in both α- and γ-phase. Specifically, $\phi_\alpha = 0.8$ rad and $\phi_\gamma = 0.68$ rad, respectively. And the direction fluctuates around ϕ_α at each step in β-phase based on (3). Moreover, the largest direction transition between two consecutive time steps is $0.23\ \pi$ between 28th and 29th second, which means only small direction change occurs in each time step. As the difference between ϕ_α and ϕ_γ is small in this example, it implies a strong temporal correlation between consecutive velocities for the node. Thus, the target direction ϕ_α effectively predicts the direction of the entire SMS movement.

2.2 Stochastic process of SMS model

Since the proposed SMS model is based on the physical law of moving objects, the smooth movement is acquired without sharp turns and sudden stop. However, as described in Sect. 1 that we also expect a mobility model to have other properties such as steady speed and uniform spacial node distribution. Therefore, we investigate the properties of SMS model based on the analysis of stochastic process.

2.2.1 Renewal process of SMS model

For proper nomenclature, random variables used to represent the process in SMS stochastic model are denoted at two levels: all random variables denoted for SMS movements are written in *upper case* and within each movement, all random variables denoted for trips for each time step are written in *normal font*. Multi-dimensional variables (e.g., random coordinates in the simulation area) are written in *bold face*. In the proposed model, all mobile nodes move independently from each other and have the identical stochastic properties, so that it is sufficient to focus on the study of stochastic process of the SMS model with respect to a specific node. Hence, we suppress the node index in the denotations of random variables for simplicity. The discrete-time parameter i indexes the ith movement of an SMS node, where $i \in \mathbb{N}_o$, and $\mathbb{N}_o$ is denoted as a countable non-negative integer space. The discrete-time parameter j indexes the jth time step within one movement of an SMS node. For discrete-time stochastic process in SMS model, all indexes are written in *normal font*. For example, $v(i, j)$ denotes node speed at jth time step within its ith movement.

For the rest of the article, we use the following denotations for *movements* and *steps* within each movement:

- SMS movement: *Movement Duration* $T(i)$ represents the time period of the ith movement from the beginning

of α-phase to the end of γ-phase; *Movement Position* $\mathbf{P}(i)$ represents the ending position of the ith movement; and $\mathcal{K}(i)$ is total number of time steps of the ith movement, where $\mathcal{K}(i) = \alpha(i) + \beta(i) + \gamma(i)$.

- Steps: *Step Position* $\mathbf{d}(i, j)$, *Step Speed* $v(i, j)$, and *Step Direction* $\phi(i, j)$ denote the ending position, speed, and direction at the jth time step of the ith movement, respectively.

As a new transition happens at the beginning time at each SMS movement, the movement can be regarded as a *recurrent* event. The movement duration $T(i)$ represents the time between the (i–1)th and the ith transition of the SMS movement. Since $T(i)$ is an i.i.d. random variable, the movement of SMS model is a *renewal process* $\{N(t); t \geq 0\}$, where $N(t)$ denotes the number of renewals by time t [31]. Without considering the pause time after each movement, the time instant S_i at which the ith renewal occurs, is given by:

$$S_i = T(1) + T(2) + \cdots + T(i), \qquad S_0 = 0, \quad i \in \mathbb{N}. \tag{6}$$

Hence, $N(t)$ is formally defined as $N(t) \triangleq \max\{i : S_i \leq t\}$. If consider that a random pause time T_p comes after each SMS movement, then we denote $\widetilde{T}(i)$ as the time between the (i–1)th and the ith transition of the SMS process, where $\widetilde{T}(i) = T(i) + T_p(i)$. Because $T_p(i)$ is an i.i.d random variable and independent from $T(i)$, $\widetilde{T}(i)$ is also an i.i.d random variable. Therefore, the consecutive movements of SMS model is a discrete-time renewal process irrespective of pause time.

2.2.2 Semi-Markov process of SMS model

Since an SMS movement consists of three consecutive moving phases and a pause p-phase, the continuous-time SMS can be represented as an iterative four-state transition process, which is shown in Fig. 2.

Let I represent the set of phases in SMS process, then $I(t)$ denotes the current phase of SMS process at time t, where $I = \{I_\alpha, I_\beta, I_\gamma, I_p\}$. Let $\{\mathcal{Z}(t); t \geq 0\}$ denote the process which makes transitions among four phases in I and $\mathcal{Y}_n$ denote the state of $\{\mathcal{Z}(t)\}$ at the epoch of its nth transition. Because the transition time between consecutive moving states in an SMS movement has a discrete uniform distribution, as shown in Fig. 2, instead of an exponential distribution. By this argument, $\{\mathcal{Z}(t)\}$ is a *semi-Markov process* [32]. This is the very reason that our mobility model is called *semi-Markov smooth* model because it can be modeled by a semi-Markov process and it complies with the physical law with smooth movement. Accordingly, $\{\mathcal{Y}_n; n \in \mathbb{N}\}$ is the four-state *embedded semi-Markov chain* of $\{\mathcal{Z}(t)\}$.

We denote P_{s1s2} as the probability that when $\{\mathcal{Y}_n\}$ enters a state $s1$, the next state that will be entered is $s2$. Further, $F_{s1s2}(t)$ denotes the cumulative distribution function (CDF) of the time to make the $s1 \rightarrow s2$ transition when the successive states are $s1$ and $s2$. Let $\mathcal{T}_{s1}$ represent the *holding-time* that the process stays at state $s1$ before making a next transition. Then we use $H_{s1}(t)$ to represent the CDF of holding-time at state $s1$, which is defined as follows [32]:

$$\begin{aligned} H_{s1}(t) &= \sum_{s2 \in I} Prob\{\mathcal{T}_{s1} \leq t | \text{next state } s2\} P_{s1s2} \\ &= \sum_{s2 \in I} F_{s1s2}(t) P_{s1s2}. \end{aligned} \tag{7}$$

According to four-state semi-Markov chain $\{\mathcal{Y}_n\}$ shown in Fig. 2, there is only uni-directional transition between two adjacent states in SMS model, such that the state transition probability $P_{s1s2} = 1$, if and only if $s1s2 \in \{I_\alpha I_\beta, I_\beta I_\gamma, I_\gamma I_p, I_p I_\alpha\}$. Under this condition, $H_{s1}(t)$ is equal to $F_{s1s2}(t)$ in the SMS model. Specifically, $F_{I_\alpha I_\beta}(t)$, $F_{I_\beta I_\gamma}(t)$ and $F_{I_\gamma I_p}(t)$ have discrete uniform distribution, while pause time T_p can follow an arbitrary distribution, denoted by $f_{T_p}(t)$. Therefore, from (7), the probability density function (pdf) of holding-time $\mathcal{T}_{s1}$ in SMS model is a discrete uniform distribution when $s1 \neq I_p$ and is $f_{T_p}(t)$ when $s1 = I_p$. Therefore, this mobility model follows a semi-Markov process because the pdf of state holding time is not exponential distribution for Markov process.

3 Stochastic properties of SMS model

Mobility model has a significant impact on both simulation-based and analytical-based study of wireless mobile networks. A deep understanding knowledge of the moving behaviors of this model is critical to properly configure the mobility parameters for a variety of network scenarios; to correctly interpret simulation results, especially for routing protocol design and evaluation; and to provide fundamental theoretical results for other mobility related analytical studies such as link and path lifetime and network connectivity analysis. Therefore, we study the stochastic properties of SMS model in this section.

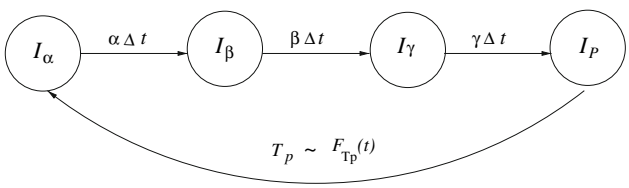

Fig. 2 Four-state transition process in SMS model

Although different mobility models lead to different mobility patterns, the stochastic properties of *movement duration*, *speed*, and *trace length* (distance) are of major interests in all mobility models because they are immediate metrics to characterize a node's movement. In fact, in every mobility model, at least two of these metrics are specified. For example, in RWP model, the mobility pattern of each movement is characterized by the trace length (distance) and speed, whereas RD model combines movement duration, speed and direction together to dominate the mobility pattern.

Based on the model assumption in Sect. 2.1, the SMS process is a renewal process, so that it is sufficient to study the stochastic properties of a single movement in SMS model by omitting the index i and use lower case j alone to identify the random variable within one SMS movement. For example, T represents the movement duration, and v_j denotes the step speed at the jth time step of this specific SMS movement.

3.1 Movement duration

In each movement, we consider the *movement duration* as the time period from the beginning of α-phase to the end of γ-phase. According to the definition of SMS model in Sect. 2.1, $T = \mathcal{K}\Delta t$ and Δt is a constant unit value, where $\mathcal{K}$ is the summation of three independent uniformly distributed random variables α, β and γ. Therefore, the duration time of one SMS movement is determined by the number of time steps $\mathcal{K}$ and movement duration follows the same probability mass function (pmf) of variable $\mathcal{K}$. So, we first derive the distribution of time steps $\mathcal{K}$ of SMS model and then, we can find the expected movement duration, $E\{T\}$. For the simplicity of denotation, we set the range of α, β, and γ as $[N_{min}, N_{max}]$ in the remaining of the paper, i.e., $\alpha_{\min} = \beta_{\min} = \gamma_{\min} = N_{min}$ and $\alpha_{\max} = \beta_{\max} = \gamma_{\max} = N_{max}$. The detailed derivation of the pmf of time steps $\mathcal{K}$ is shown in Appendix 8.1. By integrating the results of three scenarios discussed in Appendix 8.1, that is, we combine (43), (44) and (45) the pmf of time steps, $\mathcal{K}$, is obtained as:

In addition, as the duration time in each moving phase follows uniform distribution and is assumed to be equal over the range $[N_{min}, N_{max}]$, the expected value of *Movement Duration T* can be derived as follows:

$$E\{T\} = (E\{\alpha\} + E\{\beta\} + E\{\gamma\})\Delta t = \frac{3\Delta t}{2}(N_{min} + N_{max}). \tag{9}$$

Since Δt is a constant unit time, in order to simplify the presentation, Δt is normalized to unity in the rest of the article.

The distribution of movement duration can be used to determine the probability of a specific movement period as shown in Fig. 3 in which the pmf and CDF of one SMS movement duration according to different phase duration range [6, 30] s and [10, 40] s are demonstrated in Fig. 3(a) and (b), respectively.

As each phase duration in the SMS movement has a discrete uniform distribution, from (9), the average movement duration is 54 s when $[N_{min}, N_{max}] = [6, 30]$ s, and is 75 s when $[N_{min}, N_{max}] = [10, 40]$ s, respectively. Hence, in Fig. 3(a), it is clear to see that the peak value of pmf exists at time instant 54th and 75th seconds, respectively. Because the entire SMS movement duration is within the range $[3N_{min}, 3N_{max}]$ s, we can see from Fig. 3(b) that the CDF of SMS movement monotonously increases with time, and becomes 1 when the duration time reaches the maximum movement duration range, i.e., $3N_{max}$ seconds.

The knowledge of movement duration is useful to understand the dynamics of user mobility, e.g., longer movement duration means a user spends more time in moving. Upon the distribution of the SMS movement duration, we can flexibly configure the SMS model to mimic different types of mobile nodes with specific average movement duration times. Moreover, when applying the SMS model in a cellular network, it is desirable to

$$Prob\{T = k\Delta t\} = Prob\{\mathcal{K} = k\}$$
$$= \begin{cases} \dfrac{k^2 - 6k \cdot N_{min} + 3k + 9N_{min}^2 - 9N_{min} + 2}{2(N_{max} - N_{min} + 1)^3} & 3N_{min} \le k \le 2N_{min} + N_{max} \\ \dfrac{6k(N_{min} + N_{max}) - 2k^2 - 3(N_{min}^2 + N_{max}^2 + 4N_{min} \cdot N_{max} + N_{min} - N_{max}) + 2}{2(N_{max} - N_{min} + 1)^3} & 2N_{min} + N_{max} \le k \le 2N_{max} + N_{min} \\ \dfrac{k^2 - 6k \cdot N_{max} - 3k + 9N_{max}^2 + 9N_{max} + 2}{2(N_{max} - N_{min} + 1)^3} & 2N_{max} + N_{min} \le k \le 3N_{max}. \end{cases} \tag{8}$$

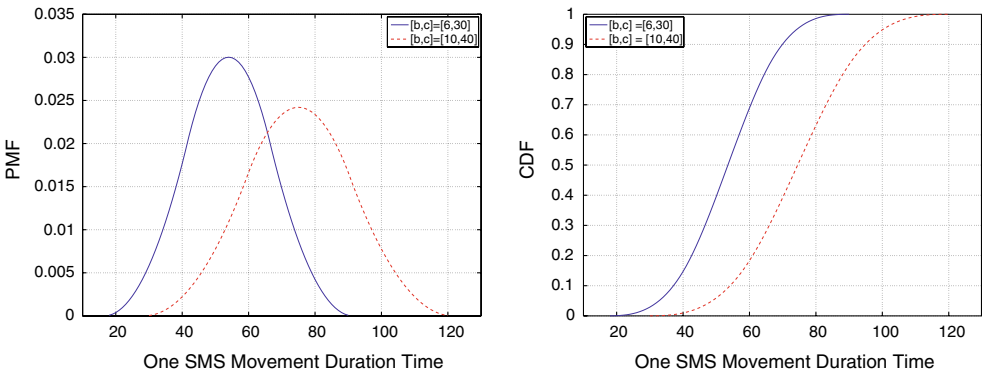

Fig. 3 The PMF and CDF of one SMS movement duration according to different phase duration ranges

(a) PMF of One SMS Movement Duration. **(b)** CDF of One SMS Movement Duration.

obtain the distribution of movement duration of mobile users for studying time-based updating schemes.

3.2 Stochastic properties of step speed

In random models, the study of stochastic properties is based on the movement process. However, being distinguished from random models, one of the main features of the SMS model is that each movement is quantized into many tiny time steps in order to capture the transient behaviors of moving objects from a *microscopic view*. Therefore, the stochastic properties of the SMS model can be characterized at the macroscopic level (i.e., movement) and microscopic level (time steps). In order to properly control the SMS model with respect to different mobility parameters for both simulation and analytical study, it is necessary to investigate the properties of SMS model on the microscopic level, which is more challenging than that on the macroscopic level.

Recall the denotations in Sect. 2.2.1, we use *step speed* to describe the speed within each time step. Therefore, we study the stochastic properties of step speed v_j, where $1 \leq j \leq N_{max}$ for each moving phase. The denotations of random variables applied for studying the stochastic properties of step speed are presented as follows.

v_α:	the target speed for α-phase.
$f_{v_\alpha}(v)$:	the pdf of target speed v_α.
v_β:	the ending step speed in β-phase.
$f_{v_\beta}(v)$:	the pdf of step speed v_β.
$v_\alpha(j)$:	the jth step speed in α-phase.
$v_\beta(j)$:	the jth step speed in β-phase.
$f_{v_{\beta(j)}}(v)$:	the pdf of jth step speed $v_\beta(j)$ in β-phase.
$v_\gamma(j)$:	the jth step speed in γ-phase.
$E_\alpha\{v\}$:	the average speed of a node in entire α-phase
$E_\beta\{v\}$:	the average speed of a node in entire β-phase
$E_\gamma\{v\}$:	the average speed of a node in entire γ-phase

3.2.1 Step speed in α-phase

From (1), the jth step speed in α-phase is represented as $v_{I_\alpha,j} = \frac{v_\alpha}{\alpha} j$. We consider two cases of time step index j with the range of α-phase duration $[N_{min}, N_{max}]$. One is the case when $j \leq N_{min}$, the other is the case when $N_{min} < j \leq N_{max}$. So that the effective α-phase duration range according to a specific time step index j is $[\max\{N_{min}, j\}, N_{max}]$. Then, the CDF of jth step speed in α-phase is derived as follows:

$$
\begin{aligned}
Pr\{v_\alpha(j) \leq v\} &= Pr\left\{\frac{v_\alpha}{\alpha} j \leq v\right\} = Pr\left\{v_\alpha \leq \frac{v \cdot \alpha}{j}\right\} \\
&= E\left\{\mathbf{1}_{\left\{v_\alpha \leq \frac{v \cdot \alpha}{j}\right\}}\right\} = \sum_{m=\max\{N_{min},j\}}^{N_{max}} E\left\{\mathbf{1}_{\left\{v_\alpha \leq \frac{v \cdot \alpha}{j}\right\}} \cdot \mathbf{1}_{\{\alpha=m\}}\right\} \\
&= \frac{1}{N_{max} - \max\{N_{min}, j\} + 1} \sum_{m=\max\{N_{min},j\}}^{N_{max}} Pr\left\{v_\alpha \leq \frac{v \cdot m}{j}\right\} \\
&= \frac{1}{N_{max} - \max\{N_{min}, j\} + 1} \sum_{m=\max\{N_{min},j\}}^{N_{max}} \int_{v_{\min}}^{\frac{v \cdot m}{j}} f_{v_\alpha}(v) dv,
\end{aligned}
\tag{10}
$$

where $v_{\min} \le v \le v_{\max}$. Here, $\mathbf{1}_{\{\cdot\}}$ is the indicator function [33]. Thus, if the event that $\left\{v_\alpha \le \frac{v\cdot\alpha}{j}\right\}$ is true, then $\mathbf{1}_{\left\{v_\alpha \le \frac{v\cdot\alpha}{j}\right\}} = 1$, otherwise $\mathbf{1}_{\left\{v_\alpha \le \frac{v\cdot\alpha}{j}\right\}} = 0$. Note, in the above equation, if $(\frac{v\cdot m}{j} > v_{\max}$ & $m < N_{max})$, then $\int_{v_{\min}}^{\frac{v\cdot m}{j}} f_{v_\alpha}(v)dv = Pr\{v_\alpha \le v_{\max} < \frac{v\cdot m}{j}\} = 1$. Moreover, as the time step index j increases, the probability $Pr\left\{v_\alpha \le \frac{v\cdot m}{j}\right\}$ decreases. Hence, the CDF of step speed in α-phase is inverse proportion to the time step j. In the special case, when $j = N_{max}$, then Eq. 10 is equivalent to the expression of CDF of the target speed v_α, i.e., the ending speed of α-phase. The average speed of a node $E_\alpha\{v\}$ in the entire α-phase is equal to the expected trace length in α-phase over the average phase duration time. Based on the description of α-phase, $E_\alpha\{v\}$ is obtained as:

$$E_\alpha\{v\} = \frac{1}{2}E\{v_\alpha\} = \frac{1}{4}(v_{\min} + v_{\max}). \tag{11}$$

Hence, for each SMS movement, the average speed of a node in the speed up phase is half of the average target speed v_α, i.e., half of the expected stable speed, selected for that movement.

3.2.2 Step speed in β-phase

For simplicity, let us denote $\widetilde{V}_j$ as $\sqrt{1-\zeta^2}\sum_{m=0}^{j-1}\zeta^{j-m-1}\widetilde{V}_m$ in (2). Then the speed at the jth step of β-phase in (2) is equivalent to $v_\beta(j) = v_\alpha + \widetilde{V}_j$. Since the summation of n independent Gaussian random variables is still a Gaussian random variable [34], $\widetilde{V}_j$ is a Gaussian random variable with zero mean and variance $\sigma_{\widetilde{V}_j} = 1-\zeta^{2j}$, i.e., $\widetilde{V}_j \sim N(0, 1-\zeta^{2j})$. In this way, $v_\beta(j)$ is the summation of two independent random variables, v_α and $\widetilde{V}_j$. Based on (Eqs. 6–38) in [34], the pdf of jth step speed in β-phase, $v_\beta(j)$ is derived as:

$$\begin{aligned} f_{v_\beta(j)}(v) &= \int_{-\infty}^{\infty} f_{v_\alpha}(v-u) f_{V_j}(u)\mathbf{1}_{\{v_{\min} \le v-u \le v_{\max}\}}du \\ &= \frac{1}{v_{\max}-v_{\min}}\int_{v-v_{\max}}^{v-v_{\min}} \frac{1}{\sqrt{2\pi}\sigma_u} e^{-\frac{u^2}{2\sigma_u^2}}du \\ &= \frac{1}{v_{\max}-v_{\min}}\int_{\frac{v-v_{\max}}{\sigma_u}}^{\frac{v-v_{\min}}{\sigma_u}} \frac{1}{\sqrt{2\pi}} e^{-\frac{u^2}{2}}du \\ &= \frac{\mathbb{G}\left(\frac{v-v_{\min}}{\sqrt{1-\zeta^{2j}}}\right) - \mathbb{G}\left(\frac{v-v_{\max}}{\sqrt{1-\zeta^{2j}}}\right)}{v_{\max}-v_{\min}}, \end{aligned} \tag{12}$$

where function $\mathbb{G}(\cdot)$ is defined as $\mathbb{G}(x) = \frac{1}{\sqrt{2\pi}}\int_{-\infty}^{x} e^{-\frac{y^2}{2}}dy$, and $\sigma_u = \sigma_{V_j} = 1-\zeta^{2j}$.

Note that there exists a non-zero probability that $\widetilde{V}_j$ has a very large magnitude for the Gaussian random variable $\widetilde{V}_j \in \mathbb{R}$. However, according to the tail of the Gaussian pdf, the probability that $\widetilde{V}_j$ is selected very far away from its mean value is considerable small. For instance, $P\{|\widetilde{V}_j - E\{\widetilde{V}_j\}| < 3\sigma_{\widetilde{V}_j}\} = 0.9973$ [34]. Since $E\{\widetilde{V}_j\} = 0$, $\widetilde{V}_j$ is mostly selected from the domain $[-3\sigma_{\widetilde{V}_j}, 3\sigma_{\widetilde{V}_j}]$ and $\sigma_{\widetilde{V}_j} = \sqrt{1-\zeta^{2j}}$ is less than 1. Thus, one can safely ignore the large values of $\widetilde{V}_j$ during the simulation. To further prevent this potential simulation abnormality, we use a threshold which is the same as $v_{\max}$ for the step speed selection in β-phase: if the new target speed is higher than $v_{\max}$ or less than 0 m/s, the speed will be reselected.

Based on above assumption, with (12), the CDF of step speed in β-phase is derived as:

$$Pr\{v_\beta(j) \le v\} = \frac{\int_0^v \mathbb{G}\left(\frac{v-v_{\min}}{\sqrt{1-\zeta^{2j}}}\right) - \mathbb{G}\left(\frac{v-v_{\max}}{\sqrt{1-\zeta^{2j}}}\right)dv}{v_{\max}-v_{\min}}. \tag{13}$$

From (13), the CDF of step speed in β-phase decreases gradually as the time step j increases. In turn, the value of $\sqrt{1-\zeta^{2j}}$ immediately approaches to 1, such that the difference of CDFs between consecutive step speeds is imperceptible. This property is distinct from that in α-phase in which according to (10), the CDF of step speed decreases as j increases. Therefore, the theoretical expressions are consistent with the designed mobility patterns in that the step speed in α-phase increases gradually and becomes stable in the entire β-phase. Because the step speed in β-phase changes on the basis of target speed v_α with a zero mean Gaussian random variable $\widetilde{V}$, upon (19), the average speed of a node in the entire β-phase is:

$$E_\beta\{v\} = E\{v_\alpha\} = \frac{1}{2}(v_{\min} + v_{\max}). \tag{14}$$

Hence, the physical meaning of (14) indicates that for each SMS movement, the average speed of a node in the middle smooth phase is just the expected stable speed selected for that movement.

3.2.3 Step speed in γ-phase

From (5), the jth step speed in γ-phase is represented as $v_\gamma(j) = v_\beta(1-\frac{j}{\gamma})$. With the same methodology of derivation in (10), the CDF of jth step speed in γ-phase is given by:

$$Pr\{v_\gamma(j) \le v\} = Pr\left\{v_\beta\left(1-\frac{j}{\gamma}\right) \le v\right\} = E\left\{\mathbf{1}_{\left\{v_\beta \le \frac{v\cdot\gamma}{\gamma-j}\right\}}\right\}$$
$$= \sum_{m=\max\{N_{min},\, j\}}^{N_{max}} E\left\{\mathbf{1}_{\left\{v_\beta \le \frac{v\cdot\gamma}{\gamma-j}\right\}} \cdot \mathbf{1}_{\{\gamma=m\}}\right\}$$
$$= \frac{1}{N_{max} - \max\{N_{min}, j\} + 1} \sum_{m=\max\{N_{min},\, j\}}^{N_{max}} Pr\left\{v_\beta \le \frac{v\cdot m}{m-j}\right\}$$
$$= \frac{1}{N_{max} - \max\{N_{min}, j\} + 1} \sum_{m=\max\{N_{min},\, j\}}^{N_{max}} \int_0^{\frac{v\cdot m}{m-j}} f_{v_\beta}(v)dv, \tag{15}$$

where $v_{\min} \le v \le v_{\max}$. $f_{v_\beta}(v)$ is the pdf of ending step speed in β-phase, and is derived by substituting β for j from (12). Note, in (15), if $\left(\frac{v\cdot m}{m-j} > v_{\max}\right)$, that is, $m < \frac{j\cdot v_{\max}}{v_{\max}-v}$. Thus, if $\left(\max\{N_{min}, j\} < m < \left\lfloor\frac{j\cdot v_{\max}}{v_{\max}-v}\right\rfloor\right)$, then $\int_{v_{\min}}^{\frac{v\cdot m}{m-j}} f_{v_\beta}(v)dv = Pr\{v_\beta \le v_{\max} < \frac{v\cdot m}{m-j}\} = 1$. Compared to the CDF of step speed in α-phase, the CDF of step speed in γ-phase is in proportion to the number of time steps j. That is the CDF of step speed in γ-phase increases as the time step j increases, which implies that step speed decreases gradually in γ-phase. The average speed of a node in entire γ-phase is:

$$E_\gamma\{v\} = \frac{1}{2}E\{v_\beta\} = \frac{1}{2}E\{v_\alpha\} = \frac{1}{4}(v_{\min} + v_{\max}). \tag{16}$$

Given the above analysis, it is evident that for each movement, the average speed in α-phase is the same as that in γ-phase, and is half of average speed in β-phase, which is the expected stable speed selected for that movement. Based on the properties of step speed of a node in each phase, we can further study the trace length, initial average speed and steady state speed distribution of the SMS model in the subsequent sections.

3.3 Trace length

We define the *trace length* as the length of actual trajectory a node travels and *distance* as the Euclidean distance between the starting position and ending position of one SMS movement. The correlation between trace length and distance of one SMS movement is dominated by the temporal correlation of velocities of the node during the movement. Especially, if the memory level parameter ζ is set 1 for step speed in (2) and step direction in (3) of β-phase, then the trajectory of an entire SMS movement is a straight line, which means that the trace length is equal to the distance in one movement. Otherwise, the distance is always smaller than the trace length as the directions in both β- and γ-phase are different from the direction in α-phase.

Figure 4 illustrates the total trace length vs. time according to three phases of one SMS movement. As shown in Fig. 4, the trace length L includes three parts, such that $L = l_\alpha + l_\beta + l_\gamma$, where l_α, l_β, l_γ are the trace length in α- β-, γ-phase, respectively. The properties of trace length of the mobility models are critical to the research in mobile wireless networks, since the trace length is closely related to the distance in SMS model. When the temporal correlation is strong, mobile nodes associated with longer trace will more easily evoke link and path failures between node pairs due to limited transmission range. Hence, the trace length has impacts on link and path stability, which in turn affects on routing protocol performance [35] and routing design issues [36–38]. Also, the stochastic properties of trance length and the corresponding distance of one SMS movement can help in location-based design schemes in mobile wireless networks, such as topology control [7, 8] and location management [39]. The stochastic properties of trace length according to three moving phases are derived as follows.

3.3.1 Trace length l_α in α-phase

With the movement time and speed, $l_\alpha = \frac{1}{2}a_\alpha \times (\alpha\Delta t)^2$. The CDF of l_α is derived as:

$$Pr\{l_\alpha \le l\} = \sum_{m=b}^{N_{max}} Pr\{v_\alpha \times \alpha \le 2l | \alpha = m\} Pr\{\alpha = m\}$$
$$= \frac{1}{N_{max} - N_{min} + 1} \sum_{m=b}^{N_{max}} Pr\left\{v_\alpha \le \frac{2l}{m}\right\}$$

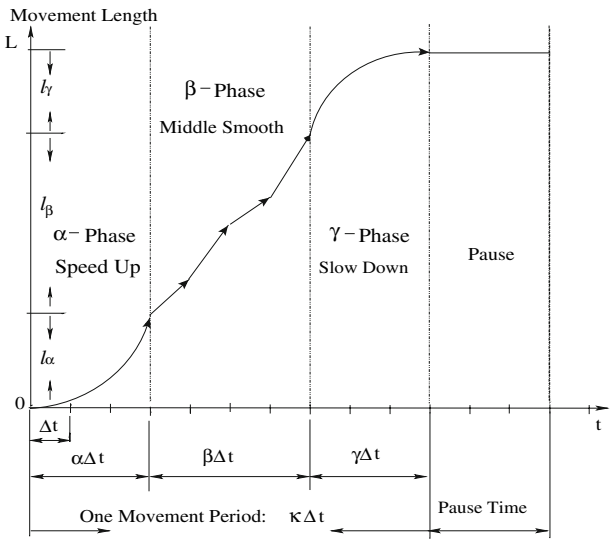

Fig. 4 Length vs. time in one SMS movement

$$= \frac{1}{N_{max} - N_{min} + 1} \sum_{m=b}^{N_{max}} \int_{v_{min}}^{\frac{2l}{m}} f_{v_\alpha}(v) dv$$
$$= \frac{2l}{(N_{max} - N_{min} + 1)} \frac{\psi(N_{max} + 1) - \psi(N_{min})}{v_{\max} - v_{\min}} - \frac{v_{min}}{v_{\max} - v_{\min}}, \quad (17)$$

where $\psi(\cdot)$ is the Psi function $\psi(n) = \frac{\Gamma'(n)}{\Gamma(n)}$ and $\Gamma(\cdot)$ is the gamma function [40]. From (17), the derivative of $Pr\{l_\alpha \le l\}$ with respect to l yields the pdf of l_α as:

$$f_{l_\alpha}(l) = \frac{2}{(N_{max} - N_{min} + 1)} \frac{\psi(N_{max} + 1) - \psi(N_{min})}{v_{\max} - v_{\min}}. \quad (18)$$

Given (17) and (18), we find that the distribution of l_α is mainly dependent on distributions of both target speed v_α and phase duration $[N_{min}, N_{max}]$. Since both target speed and phase duration are uniformly distributed, the distribution of l_α is solely dominated by the range of target speed $[v_{\min}, v_{\max}]$ and phase duration $[N_{min}, N_{max}]$.

3.3.2 Trace length l_β in β-phase

The travel distance in the entire β-phase can be obtained as:

$$l_\beta = v_\alpha \beta \Delta t + \sqrt{1 - \zeta^2} \sum_{n=1}^{\beta} \sum_{m=0}^{n-1} \zeta^{n-m-1} \widetilde{V}_m \Delta t, \quad (19)$$

which can be simplified as a function of two independent random variables, that is $l_\beta = l'_\beta + \widetilde{l}$, where $l'_\beta = v_\alpha \cdot \beta$, and $\widetilde{l} = \sqrt{1 - \zeta^2} \sum_{n=1}^{\beta} \sum_{m=0}^{n-1} \zeta^{n-m-1} \widetilde{V}_m$. Because random variable α and β have identical distributions, we have $l'_\beta = 2l_\alpha$. Hence, the pdf of l'_β is derived as $f_{l'_\beta}(l) = \frac{1}{2} f_{l_\alpha}(\frac{l}{2})$. On the other hand, we observed that $\widetilde{l}$ is a superposed Gaussian random variable, i.e., $\widetilde{l} \sim N(0, \sigma_l^2)$. The variance σ_l^2 of $\widetilde{l}$ is derived as:

$$\sigma_{\widetilde{l}}^2 = (1 - \zeta^2) \sum_{m=1}^{\beta} \left(\frac{1 - \zeta^n}{1 - \zeta} \right)^2. \quad (20)$$

Note that, for a Gaussian random variable $\widetilde{l}$, $P\{|\widetilde{l} - E\{\widetilde{l}\}| < 3\sigma_l\} = 0.9973$ [34]. Based on the same argument on the effective range of jth step speed $v_\beta(j)$ in β-phase discussed in Sect. 3.2.2, we assume that the effective range of $\widetilde{l}$ is $[N_{min} \cdot \max\{v_{\min} - 3\sigma_l, 0\}, c \cdot (v_{\max} + 3\sigma_l)]$. Through the same methodology for deriving the pdf of step speed in β-phase in (12), the pdf of l_β is derived as:

$$\begin{aligned} f_{l_\beta}(l) &= \int_{-\infty}^{\infty} f_{l'_\beta}(l-u) f_l(u) \mathbf{1}_{\{v_{\min} \cdot N_{min} \le l-u \le v_{\max} \cdot N_{max}\}} du \\ &= \int_{-\infty}^{\infty} \frac{1}{2} f_{l_\alpha}\left(\frac{l-u}{2}\right) f_l(u) \mathbf{1}_{\{v_{\min} \cdot N_{min} \le l-u \le v_{\max} \cdot N_{max}\}} du \\ &= \frac{1}{(N_{max} - N_{min} + 1)} \frac{\psi(N_{max} + 1) - \psi(N_{min})}{v_{\max} - v_{\min}} \int_{\frac{l - v_{\max} \cdot N_{max}}{\sigma_l}}^{\frac{l - v_{\min} \cdot N_{min}}{\sigma_l}} \frac{1}{\sqrt{2\pi}} e^{-\frac{u^2}{2}} du \\ &= \frac{1}{(N_{max} - N_{min} + 1)} \frac{\psi(N_{max} + 1) - \psi(N_{min})}{v_{\max} - v_{\min}} \cdot \left(\mathbb{G}\left(\frac{l - v_{\min} \cdot N_{min}}{\sigma_l} \right) - \mathbb{G}\left(\frac{l - v_{\max} \cdot N_{max}}{\sigma_l} \right) \right). \end{aligned} \quad (21)$$

Because the distribution of l'_β is solely dominated by the distribution of l_α, given (21), the distribution of β-phase trace length l_β is dependent on the distributions of both l_α, which in turn characterized by the speed range $[v_{\min}, v_{\max}]$, phase duration $[N_{min}, N_{max}]$, and the memorial parameter ζ.

3.3.3 Trace length l_γ in γ-phase

Similar to α-phase, $l_\gamma = -\frac{1}{2} a_\gamma \times (\gamma \Delta t)^2$. By using the same methodology for deriving CDF and pdf of l_α, we have

$$Pr\{l_\gamma \le l\} = \frac{1}{N_{max} - N_{min} + 1} \sum_{m=N_{min}}^{N_{max}} \int_{v_{\min}}^{\frac{2l}{m}} f_{v_\beta}(v) dv, \quad (22)$$

and

$$f_{l_\gamma}(l) = \frac{2}{(N_{max} - N_{min} + 1)} \sum_{m=N_{min}}^{N_{max}} \frac{1}{m} f_{v_\beta}\left(\frac{2l}{m}\right), \quad (23)$$

where $f_{v_\beta}(v)$ is the pdf of ending step speed in β-phase, which is derived by substituting β for j from (12).

From (22) and (23), it is clear that the distribution of l_γ is mainly dependent on distributions of both ending speed v_β in β-phase and phase duration $[N_{min}, N_{max}]$.

So far we have analyzed the stochastic properties of *movement duration*, *step speed*, and *trace length* of the proposed SMS mobility model. These results can give a deep understanding of the behaviors of this model. Next we study the steady state features of the model.

4 Steady state analysis

For large-scale wireless networks, the moving behaviors of mobile nodes at steady state predominate the performance evaluation. During the simulation, when the random process of a mobility model reaches the steady state, trace file and the corresponding simulation results are reliable for the performance evaluation. On the other hand, analytical study also requires the steady state distribution of the interested parameter for deriving accurate theoretical expressions. Therefore, we focus on the time stationary distribution of SMS model and steady state analysis of speed in SMS model to demonstrate that there is no speed decay problem. Then, we will demonstrate the nodal distribution at steady state.

4.1 Time stationary distribution

Recall the renewal process described in Sect. 2.2 Let $E\{\mathcal{T}_{s1}\}$ be the mean value of holding-time that the semi-Markov process spends at state $s1$ before making a next transition, that is

$$E\{\mathcal{T}_{s1}\} = \int_0^\infty t\, dH_{s1}(t). \tag{24}$$

Then $E\{\mathcal{T}_{s1s1}\}$ denotes the mean recurrence time, i.e., the average first recurrent time after leaving state $s1$ [32]. It is known that for an irreducible semi-Markov process $\{\mathcal{U}(t)\}$, if $E\{\mathcal{T}_{s1s1}\} < \infty$, then for any state $s1$, the limiting probability P_{s1} exists and is independent of the initial state, for example $\mathcal{U}(0) = u$, that is,

$$P_{s1} = \lim_{t\to\infty} Prob\{\mathcal{U}(t) = s1 \,|\, \mathcal{U}(0) = s2\} = \frac{E\{\mathcal{T}_{s1}\}}{E\{\mathcal{T}_{s1s1}\}}. \tag{25}$$

According to our SMS model, the embedded semi-Markov chain $\{\mathcal{Y}_n\}$ is *irreducible* since each state is reachable from any other states. Because $\{\mathcal{Y}_n\}$ is irreducible, the semi-Markov process $\{\mathcal{Z}(t)\}$ is also irreducible. Furthermore, $\{\mathcal{Y}_n\}$ is positive recurrent because it is an irreducible semi-Markov chain with finite states. By applying (24) into $\{\mathcal{Y}_n\}$, we have $E\{T_{s1}\} = E\{\alpha\} = \frac{N_{min}+N_{max}}{2}$, when $s1 \neq I_p$ and $E\{T_{I_p}\} = E\{T_p\}$. Therefore, for any state $s1$ of $\{\mathcal{Y}_n\}$, $E\{\mathcal{T}_{s1s1}\} = E\{\alpha\} + E\{\beta\} + E\{\gamma\} + E\{T_p\} < \infty$, so the limiting probability of each state exists in the SMS model. In turn, the time stationary distribution P_υ for each state υ exists in the SMS model according to (25). Let $\pi = (\pi_\alpha, \pi_\beta, \pi_\gamma, \pi_p)$ denote the time stationary distribution of SMS stochastic process. By combining (24) and (25), we derive the time stationary distribution for each phase in the SMS model as following:

$$\pi_m = \lim_{t\to\infty} Prob\{I(t) = I_m \in I\} = \frac{E\{T_m\}}{E\{T\} + E\{T_p\}}. \tag{26}$$

The time stationary properties obtained in the above equation will be used in evaluating the average speed at the initial state so that we can further prove that there is no speed decay in the SMS model. We have studied the stochastic properties of step speed v_j, where $1 \le j \le N_{max}$ for each phase in Sect. 3.2. Now we are interested in the speed distribution at steady state in Sect. 4.2 and average speed in Sect. 4.3. The nodal distribution will be discussed in Sect. 4.4.

4.2 Speed distribution at steady state

In order to find the average speed at steady state, we derive the speed distribution first. Let $\mathcal{M}(t)$ and $\mathcal{M}_p(t)$ denote the total number of time steps that a node travels and pauses from the beginning till time t, respectively. Recall, $N(t)$ represents the number of renewal movements by time t. Hence, $\mathcal{M}_p(t) = \sum_{i=1}^{N(t)} T_p(i)$. If we consider the last incomplete movement, then $\sum_{i=1}^{N(t)} T(i) \le \mathcal{M}(t) < \sum_{i=1}^{N(t)+1} T(i)$. We denote v_{ss} as the steady-state speed of the SMS model. Then, $F_{v_{ss}}(v)$ of v_{ss} can be derived from the limiting fraction of time when step speeds are less than v, as the entire simulation time t approaches to infinity. When $t \to \infty$, $N(t) \to \infty$, such that one can safely omit the impact of fraction time in the last incomplete movement.

The formal derivation of $F_{v_{ss}}(v)$is shown in the Appendix 8.2. Here, we present the final result of $F_{v_{ss}}(v)$ as:

$$\begin{aligned} &Pr\{v_{ss} \le v\} \\ &= \frac{1}{E\{T\}+E\{T_p\}} \cdot \left[E\{T_p\} + \frac{1}{N_{max}-N_{min}+1} \sum_{m=N_{min}}^{N_{max}} \sum_{j=1}^{m} \cdot \left(\int_{v_{\min}}^{\frac{v \cdot m}{j}} f_{v_\alpha}(v)dv + \int_0^{v} f_{v_\beta(j)}(v)dv + \int_0^{\frac{v \cdot m}{m-j}} f_{v_\beta}(v)dv \right) \right]. \end{aligned} \tag{27}$$

Corresponding to (30), the expectation of steady state speed $E\{v_{ss}\}$ is also composed of four distinct components

4.3 Average speed at steady state

A well-known problem of RWP model is that it fails to provide a steady average speed which decreases over time [17]. Thus, we examine whether there exists the speed decay phenomenon in the SMS model for which we need to obtain both the initial average speed $E\{v_{ini}\}$ and the average steady state speed $E\{v_{ss}\}$. More importantly, the average speed at steady state should be independent of initial speed and locations [25].

The initial state of the SMS model is chosen based on the time stationary distribution $\pi = (\pi_\alpha, \pi_\beta, \pi_\gamma, \pi_p)$ of the SMS process in Sect. 4.1. From (11), (14), (16), and (26), the initial average speed of the SMS model is derived as:

$$\begin{aligned} E\{v_{ini}\} &= E\{E\{v_{ini} \mid I_m\}\} \\ &= E_\alpha\{V\}\pi_\alpha + E_{I_\beta}\{V\}\pi_\beta + E_{I_\gamma}\{V\}\pi_\gamma + 0 \cdot \pi_p \\ &= \frac{\frac{1}{2}E\{v_\alpha\}(E\{\alpha\} + 2E\{\beta\} + E\{\gamma\})}{E\{T\}+E\{T_p\}}. \end{aligned} \tag{28}$$

By differentiating the CDF of steady state speed v_{ss} from (27) with respect to v, it is observed that the pdf of v_{ss} consists of four distinct components according to each state of $\{\mathcal{Y}_n\}$:

$$f_{v_{ss}}(v) = f_{v_{ss}}^{I_\alpha}(v) + f_{v_{ss}}^{I_\beta}(v) + f_{v_{ss}}^{I_\gamma}(v) + f_{v_{ss}}^{I_p}(v) \tag{29}$$

The four components of $F_{v_{ss}}(v)$ in (29) are given by:

$$f_{v_{ss}}(v) = \begin{cases} \frac{\frac{1}{N_{max}-N_{min}+1}\sum_{m=N_{min}}^{N_{max}}\sum_{j=1}^{m}\frac{m}{j}f_{v_\alpha}\left(\frac{v \cdot m}{j}\right)}{E\{T\}+E\{T_p\}} & v \text{ of } I_\alpha \\ \frac{\frac{1}{N_{max}-N_{min}+1}\sum_{m=N_{min}}^{N_{max}}\sum_{j=1}^{m}f_{v_\beta(j)}(v)}{E\{T\}+E\{T_p\}} & v \text{ of } I_\beta \\ \frac{\frac{1}{N_{max}-N_{min}+1}\sum_{m=N_{min}}^{N_{max}}\sum_{j=1}^{m}\frac{m}{m-j}f_{v_\beta}\left(\frac{v \cdot m}{m-j}\right)}{E\{T\}+E\{T_p\}} & v \text{ of } I_\gamma \\ \frac{E\{T_p\}\delta(v)}{E\{T\}+E\{T_p\}} & v \text{ of } I_p \end{cases}. \tag{30}$$

with regards to each state of embedded semi-Markov chain $\{\mathcal{Y}_n\}$, which are derived in Appendix 8.3. The result is

$$E_u\{v_{ss}\} = \begin{cases} \frac{\frac{1}{2}E\{v_\alpha\}(1+E\{\alpha\})}{E\{T\}+E\{T_p\}} & u \in I_\alpha \\ \frac{E\{v_\alpha\}E\{\beta\}}{E\{T\}+E\{T_p\}} & u \in I_\beta \\ \frac{\frac{1}{2}E\{v_\alpha\}(E\{\gamma\}-1)}{E\{T\}+E\{T_p\}} & u \in I_\gamma \\ 0 & u \in I_p. \end{cases} \tag{31}$$

Thus, the average speed at steady state, $E\{v_{ss}\}$ of the SMS model can be obtained by combining each item in (31):

$$\begin{aligned} E\{v_{ss}\} &= E_\alpha\{v_{ss}\} + E_\beta\{v_{ss}\} + E_\gamma\{v_{ss}\} + E_{I_p}\{v_{ss}\} \\ &= \frac{\frac{1}{2}E\{v_\alpha\}(E\{\alpha\} + 2E\{\beta\} + E\{\gamma\})}{E\{T\}+E\{T_p\}}. \end{aligned} \tag{32}$$

By comparing (28) with (32), we showed that the initial average speed is exactly same as average steady state speed in SMS process, i.e., $E\{v_{ini}\} = E\{v_{ss}\}$. Furthermore, since the step speed is selected independently from the number of time steps in each phase of one movement, our analytical result of average steady state speed in the SMS model is consistent with which proved by Yoon [25]: there is no speed decay phenomenon in mobility model as long as the speed and time metric for each trip are selected independently. Therefore, we proved that there is no speed decay problem for arbitrary starting speed in SMS model.

4.4 Spatial node distribution

Another problem with RWP model is that it has non-uniform node distribution, given that the initial distribution is uniform. In this section, we will prove that the SMS model with border wrap has uniform node distribution all the time and validate our results through simulations.

Here, we consider the border effect on the SMS model. When a mobile node reaches a boundary of a

two-dimensional simulation region, it wraps around and reappears instantaneously at the opposite boundary in the same direction to avoid biased effects on simulation results.

Now we study the spatial node distribution of the SMS model with border wrap by focusing on the successive movements of a single mobile node. Consider a mobile node in an SMS movement, there is a total $\mathcal{K}(i)$ time steps in a node's ith movement. Then the mobility at the jth time step of its ith movement is characterized by a triplet $(\mathbf{d}(i,j), v(i,j), \phi(i,j))$. Hence, the complete discrete-time process of the SMS node according to its ith movement is defined as: $\{\mathbf{d}(i,j), v(i,j), \phi(i,j)\}_{1\le j\le \mathcal{K}(i)}$. At first, we analyze the node distribution during the first SMS movement, i.e., $i = 1$. For a simple representation, we suppress the movement index i in the denotations of random variables, and normalize the size of the simulation region to $[0,1)^2$. For instance, $\mathbf{d}(j)$ denotes the ending position after the jth time step of the first movement, where $\mathbf{d}(j) = (X_j, Y_j)$. Then $\mathbf{d}(j)$ with border wrap on $[0,1)^2$ [21] is represented by:

$$\mathbf{d}(j) = \begin{cases} X_j = X_{j-1} + v_j\cos(\phi_j) - \lfloor X_{j-1} + v_j\cos(\phi_j)\rfloor \\ Y_j = Y_{j-1} + v_j\sin(\phi_j) - \lfloor Y_{j-1} + v_j\sin(\phi_j)\rfloor, \end{cases} \tag{33}$$

where $\lfloor\cdot\rfloor$ is the floor function. According to the target direction ϕ_α of the first movement, the jth step direction $\phi_j = \phi_\alpha + \psi_j$, where ψ_j is the *relative direction* between ϕ_α and direction at the jth time step, which ranges in $[0, 2\pi)$. Hence, ψ_j is constant in both α-phase and γ-phase and varies in β-phase. Based on (3), ψ_j is derived as follows:

$$\psi_j = \begin{cases} 0 & 1\le j\le \alpha \\ \sqrt{1-\zeta^2}\sum_{m=0}^{j-\alpha-1}\zeta^{j-\alpha-m-1}\widetilde{\phi}_m & \alpha+1\le j\le \alpha+\beta \\ \sqrt{1-\zeta^2}\sum_{m=0}^{\beta}\zeta^{\beta}\widetilde{\phi}_m & \alpha+\beta+1\le j\le \mathcal{K}. \end{cases} \tag{34}$$

Consider that ϕ_j is also within the range $[0, 2\pi)$, then we have

$$\phi_j = \phi_\alpha + \psi_j - 2\pi\left\lfloor\frac{\phi_\alpha+\psi_j}{2\pi}\right\rfloor. \tag{35}$$

At time $t = 0$, the node begins to move from the initial position $\mathbf{P}(0) = (X_0, Y_0)$, at the speed with v_1 along the step direction ϕ_1, where ϕ_1 is equal to the target direction ϕ_α. Based on a specific value $\mathbf{P}(0)$ and ϕ_α, the complete discrete-time process of its first movement is characterized by $\{v_j, \psi_j\}_{1\le j\le \mathcal{K}}$. Assume that the movement pattern $\{v_j, \psi_j\}_{1\le j\le \mathcal{K}}$ is deterministic, then we have the following lemma.

Lemma 1 *In the SMS model, if the initial position* $\boldsymbol{P}(0)$ *and the first target direction* ϕ_α *of the mobile node are chosen independently and uniformly distributed on* $[0,1)^2 \times [0, 2\pi)$ *at time* $t = 0$*, then the location and direction of the node remain uniformly distributed all the time.*

Proof Our proof of Lemma 1 is based on the result of Lemma 2.3 and the methodology for proving Lemma 4.1 in [21]. According to Lemma 2.3 of [21], for all $x \in [0, 1)$ and $a \in (-\infty, \infty)$,

$$\int_0^1 \mathbf{1}_{\{u+a-\lfloor u+a\rfloor < x\}} du = x. \tag{36}$$

As the node begins to move, with (33) and (36), the joint probability of ending position and direction of the first step movement is derived as:

$$\begin{aligned} &Pr(X_1 < x_1, Y_1 < y_1, \phi_1 < \theta) \\ &= Pr(X_1 < x_1|\phi_1 < \theta)\cdot Pr(Y_1 < y_1|\phi_1 < \theta)\cdot Pr(\phi_1 < \theta) \\ &= \frac{1}{2\pi}\int_{\phi_1=0}^{\theta}\left(\int_{x_0=0}^{1}\mathbf{1}_{\{x_0+v_1\cos(\phi_1)-\lfloor x_0+v_1\cos(\phi_1)\rfloor < x_1\}}dx_0\right. \\ &\quad\left.\cdot\int_{y_0=0}^{1}\mathbf{1}_{\{y_0+v_1\sin(\phi_1)-\lfloor y_0+v_1\sin(\phi_1)\rfloor < y_1\}}dy_0\right)d\phi_1 \\ &= \frac{x_1 y_1\theta}{2\pi}, \end{aligned} \tag{37}$$

where $x_1, y_1 \in [0, 1)$ and $\theta \in 2\pi$. The above result shows that $(\mathbf{d}(1), \phi_1)$ is uniformly distributed on $[0, 1)^2 \times [0, 2\pi)$. Since $\psi_j = 0$ for each step movement in α-phase, by following the same way of derivation in (37), we conclude that the ending position and direction for each step movement in α-phase are in turn uniformly distributed on $[0, 1)^2 \times [0, 2\pi)$.

For each step movement in β-phase and γ-phase, where $\psi_j \neq 0$, based on (35) and (36) and the result from (32) of [21], the probability $Pr(\phi_j < \theta)$ is derived as:

$$\begin{aligned} Pr(\phi_j < \theta) &= \frac{1}{2\pi}\int_0^{2\pi}\mathbf{1}_{\left\{\phi_\alpha+\psi_j-2\pi\left\lfloor\frac{\phi_\alpha+\psi_j}{2\pi}\right\rfloor < \theta\right\}}d\phi_\alpha \\ &= \int_0^1 \mathbf{1}_{\left\{u+\frac{\psi_j}{2\pi}-\left\lfloor u+\frac{\psi_j}{2\pi}\right\rfloor < \frac{\theta}{2\pi}\right\}}du = \frac{\theta}{2\pi}, \end{aligned} \tag{38}$$

where $u = \frac{\phi_\alpha}{2\pi}$, and $\alpha + 1 \le j \le \mathcal{K}$. Hence, for the first step movement in β-phase, i.e., $j = (\alpha + 1)$, we have

$$\begin{aligned} &Pr(X_{\alpha+1} < x_{\alpha+1}, Y_{\alpha+1} < y_{\alpha+1}, \phi_{\alpha+1} < \theta) \\ &= \frac{1}{2\pi}\int_{\phi_\alpha=0}^{\theta}\mathbf{1}_{\left\{\phi_\alpha+\psi_{\alpha+1}-2\pi\left\lfloor\frac{\phi_\alpha+\psi_{\alpha+1}}{2\pi}\right\rfloor < \theta\right\}}\cdot \\ &\quad\left(\int_0^1\mathbf{1}_{\{x_\alpha+v_{\alpha+1}\cos(\phi_{\alpha+1})-\lfloor x_\alpha+v_{\alpha+1}\cos(\phi_{\alpha+1})\rfloor < x_{\alpha+1}\}}dx_\alpha\right. \end{aligned}$$

$$\cdot \int_0^1 \mathbf{1}_{\{y_\alpha + v_{\alpha+1}\sin(\phi_{\alpha+1}) - \lfloor y_\alpha + v_{\alpha+1}\sin(\phi_{\alpha+1})\rfloor < y_{\alpha+1}\}} dy_\alpha \Big) d\phi_\alpha = \frac{x_{\alpha+1} y_{\alpha+1}\theta}{2\pi}. \quad (39)$$

Given the result of (39), $(\mathbf{d}(\alpha+1), \phi_{\alpha+1})$ is also uniformly distributed on $[0,1)^2 \times [0, 2\pi)$. Through the induction argument, we directly prove that for the successive step movements in β-phase and γ-phase, the uniform distribution always holds. Therefore, we conclude that the position and direction of the node are always uniformly distributed during the first movement. Since pause time does not affect the spatial node distribution in our SMS model, by induction, the uniform node distribution holds for the entire ith movement. Then, the ending position of the ith movement $\mathbf{P}(i)$ is uniformly distributed over $[0,1)^2$. Because SMS process is a renewal process, according to the stochastic property of renewal process, the position in the entire $(i+1)$th movement is also uniformly distributed. Hence, we complete the proof of Lemma 1. □

5 Simulation results

In this section, we validate the analytical results in previous section by ns-2 simulations, along with the evaluation of effects of phase duration time and pause time.

5.1 Assumptions and parameters

We integrate our SMS model into the *setdest* of ns-2 simulator [41], which currently provides both an original and a modified version of RWP model [25]. Each scenario in our simulation contains 1000 nodes moving independently in a square simulation region with size [0, 1500) m × [0, 1500) m during a time period of 1000 s. Then, 30 realizations of each scenario are made through Monte Carlo simulation. Since pause time dose not have a significant effect on the built-in RWP model [17], for comparison of average speed and node distribution demonstrated later in Sect. 4.4, we set zero pause time for both models. According to the built-in RWP model, the speed range for all scenarios is [0, 20] m/s. For the SMS model, we set the unit time slot Δt as 1 s and the memory parameter ζ as 0.5. The speed range of target speed v_α in the SMS model is considered in the range of [0, 20] m/s, so that $E\{v_\alpha\}$ = 10 m/s. In real life, it normally takes at least 6 s for a car to accelerate its speed from 0 to 20 m/s. Hence, for simulation in the SMS model, when the target speed v_α is selected close to 20 m/s, we consider at least six time steps for speed acceleration. Therefore, the range of phase duration time $[N_{min}, N_{max}]$ is selected either from [6, 30] s or [10, 40] s.

Note, as the speed/direction in each time step of β-phase are affected by a Gaussian random variable, there exists a very small non-zero probability that speed/direction may have a very large value in some time step. To avoid this unwanted event, we set a threshold $v_{\max}$ for the speed and a threshold $\pi/2$ for the direction change between two consecutive steps, respectively. If the new calculated value of speed/direction is larger than the threshold, we reselect that value.

5.2 Average speed

According to the original RWP model in ns-2, all nodes start to move at the initial time, which is named *strategy*-1 in our evaluation. To be consistent with the simulation strategy for the original RWP model, we let all nodes in the SMS model start to move from the first step of α-phase. Moreover, each phase duration time is in range of [6, 30] s. Given the simulation condition of zero pause time and $E\{\alpha\} = E\{\beta\} = E\{\gamma\} = 18$ s, from (32), the theoretical result of $E\{v_{ss}\}$ of SMS model is obtained as: $E\{v_{ss}\} = \frac{2}{3}E\{v_\alpha\} = 6.7$ m/s. Both simulation and theoretical results of average speed vs. a time period of 1000 s are shown in Fig. 5, from which we can see that after the first 200 s, the average speed of the SMS model with strategy-1 converges to the expected steady state speed 6.7 m/s and stabilizes at that level, which perfectly matches the theoretical result, whereas the average speed of RWP model continues decreasing with the simulation time.

With the modified RWP model [25], initial locations and speeds of the nodes are chosen from the steady state distributions directly, namely *strategy-2* [22, 42, 43]. By this way, the steady state of RWP process is immediately reached at the beginning of the simulation when $V_{\min} >$ 0 m/s. Correspondingly, for SMS model, we choose an

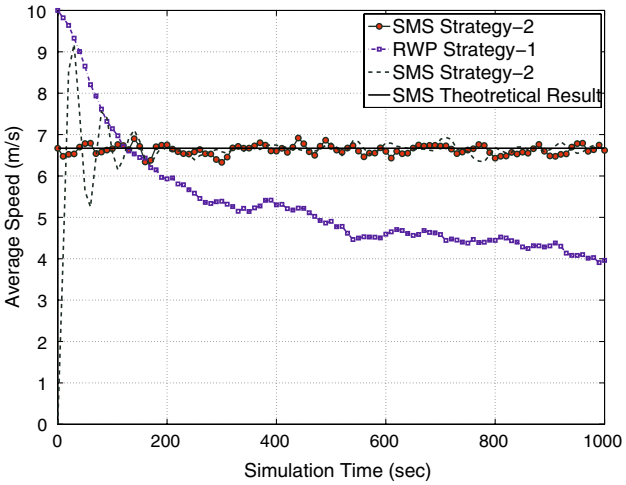

Fig. 5 Average speed vs. simulation time

initial state with a probability according to the time stationary distribution of the SMS process, $\pi = (\pi_\alpha, \pi_\beta, \pi_\gamma, \pi_p)$ in (26). Specifically, if the initial phase of a node is β-phase or γ-phase, the node will choose a random initial step speed, as $v_{\alpha+1}$ for the first step in β-phase, or $v_{\beta+1}$ for the first step in γ-phase, which is uniformly distributed over $[v_{\min}, v_{\max}]$. In Fig. 5, we can see the average speed of the SMS model according to *strategy*-2 is stable right from the start of simulation. As we expected, the average speed through *strategy*-2 has the same expected steady state speed 6.7 m/s as that obtained from *strategy*-1. Since the average speeds of the SMS model obtained through both strategies do not decay over time regardless of initial speed, the simulation results are consistent with our analytical proof shown in Sect. 4.

5.2.1 *Effect of phase duration time*

Here we want to observe the effects of the duration time of each phase on steady state speed $E\{v_{ss}\}$ in SMS model. Interestingly, based on our analytical result of $E\{v_{ss}\}$ in (32), the average speed at steady state is independent of phase duration time, if the range for each moving phase duration is same, regardless of the interval selection of the range. That is, if $E\{\alpha\} = E\{\beta\} = E\{\gamma\}$ and without pause time, the average speed at steady state in SMS model can always be evaluated as: $E\{v_{ss}\} = \frac{2}{3}E\{v_\alpha\}$. To validate our theoretical result, we simulate two scenarios according to phase duration time, [6, 30] s and [10, 40] s, respectively. Simulation results based on these two scenarios are shown in Fig. 6.

We can observe from Fig. 6 that the average speed with *strategy*-2 converges to the same expected steady state value 6.7 m/s since the beginning of the simulation. By simulation through strategy-1, the average speed based on the range of [6, 30] s converges to the steady state faster than that with the range of [10, 40] s due to its shorter average movement duration time. In fact, the longer the phase duration time, the longer time is taken for the average speed to converge. We observe that after the first 300 s, average speeds of these two scenarios with both strategies (1 and 2) are asymptotic to the same expected steady state value. Thus, the theoretical proof of $E\{v_{ss}\}$ in (32) is validated by simulations.

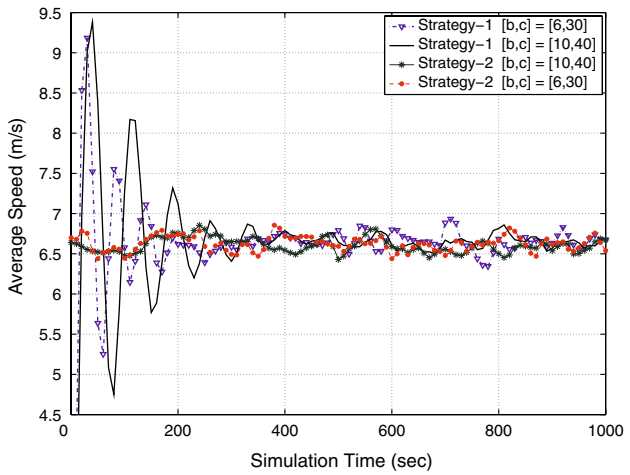

Fig. 6 Average speed vs. phase duration time

5.2.2 *Effect of pause time*

In the proposed SMS model, pause time is the time interval between any two consecutive movements. Let's look at the impact of pause time on the expected steady state speed. Here, we allow SMS nodes to pause for a random time t_P with a mean value $E\{T_p\}$ after each movement. According to (26), the stationary pause phase probability π_p is given by $\pi_p = \frac{E\{T_p\}}{E\{T\}+E\{T_p\}}$. Based on (32), for the phase duration time selected from [6, 30] s, $v \in [0, 20]$ m/s, the effect of pause time with regards to the stationary pause phase probability π_p, and steady state speed $E\{v_{ss}\}$ are shown in Table 2.

Table 2 demonstrates that as $E\{T_p\}$ increases, π_p increases monotonously, whereas $E\{v_{ss}\}$ decreases. Especially, the downtrend of $E\{v_{ss}\}$ is more evident when $E\{T_p\}$ is small. For instance, when $E\{T_p\} = 60$ s, and π_p is equal to 0.53, i.e., the pause phase becomes a dominant time period in a movement. Correspondingly, $E\{v_{ss}\} =$ 3.16 m/s which drops more than half of average speed for $E\{T_p\} =$ 0 s. According to the numerical results shown in Table 2, we find that for SMS model, there always exists a stable average speed at steady state for arbitrary pause time. Therefore, our proposed SMS model eliminates the speed decay problem regardless of pause time.

5.3 Smooth movements

The SMS model is designed by following the physical law of moving objects in order to fulfill the requirement of smooth movements, which is the second desired feature of the SMS model introduced in Sect. 1. Thus, there is no unrealistic behaviors such as sharp turns and sudden stops in this model. Here we compare the *distance* which is the Euclidean distance between the current position and the starting position during one movement, with the *trace length* which is the length of actual trajectory a node travels during one movement. Different from all macroscopic mobility models, such as RD and RWP model, because direction changes within one SMS movement, the distance is not larger than the trace length. By observing distance evolution during one movement, people can

Table 2 Effect of pause time on average speed

$E\{T_p\}$ (s)	0	10	20	30	40	50	60
π_p	0	0.16	0.27	0.36	0.43	0.48	0.53
$E\{\ v_{ss}\ \}$ (m/s)	6.67	5.63	4.86	4.29	3.83	3.46	3.16

indirectly tell the corresponding moving trajectory. Specifically, if the distance increases monotonously, it implies that the node travels forward with a smooth trace. In contrast, if the distance decreases at some time, it means that the node turns backward during the movement, that is a sharp turn event occurs. In the third case, if the distance is relative stable for some time interval, then we can tell that the node is traveling along a circle trajectory, where the starting position is the center of the circle.

The simulation results of both trace length and distance of an SMS movement are shown in Fig. 7, where $\alpha = 16$ s, $\beta = 12$ s, and $\gamma = 17$ s. We can see that both trace length and distance increase exponentially in both α-phase and γ-phase, due to the speed acceleration and deceleration, respectively. Furthermore, the trace length l_α is equivalent to the distance, due to the constant direction ϕ_α in α-phase. In β-phase, the trace length increases linearly, whereas the uptrend of the distance fluctuates because of the change of direction at every time step. Since the direction ϕ_γ dose not vary in γ-phase, both the trace length and the distance within γ-phase increase. And the difference between ϕ_α and ϕ_γ directly determines the difference between the trace length and distance in γ-phase. Moreover, as the trace length is the upper bound of the distance, the equality holds when the node moves along a straight line during an entire movement. From Fig. 7, the distance monotonously increases during the entire movement period. Therefore, we conclude that *the mobility trace in SMS model is smooth without sharp turns*.

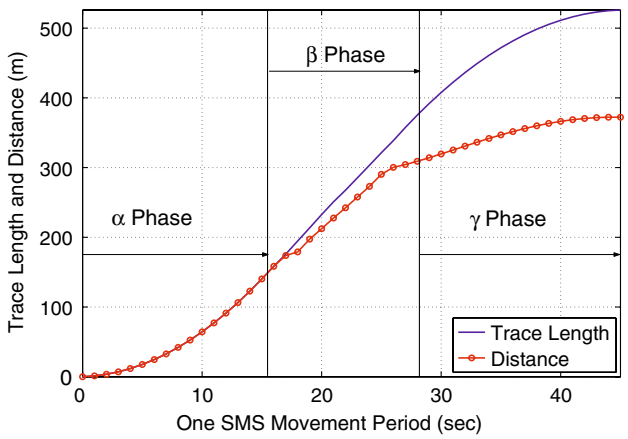

Fig. 7 Distance and trace length

5.4 Uniform node distribution

We compare the spatial node distribution of the SMS model with the RWP model to validate our proof through simulation results. For both models, we deploy 1000 nodes uniformly distributed in the simulation region at the initial time. Then, we sample the spatial node position at the 500th and the 1000th second for the SMS model, and at the 1000th second for the RWP model, respectively. A top view of two-dimensional spatial node position of the RWP and the SMS models are shown in Fig. 8.

According to Fig. 8(a), it is clear that the node density with RWP model is maximum at the center of the region, while it is almost zero at the vicinity of the simulation boundary. In contrast, from Fig. 8(b) and (c), the node density of the SMS model at the two sampling time instants are similar and mobile nodes are equally located within the simulation region. Since 500th second is the middle stage of the simulation period and 1000th second is the ending time of the simulation, both snapshots of SMS model demonstrate a uniform node distribution. Therefore, we verified our proof in Lemma 1 that the SMS model with border wrap has uniform spatial node distribution.

Since all mobile nodes travel independently and follow the same movement pattern in the SMS model, according to Lemma 1, we conclude that if the positions of all nodes in the first movement are uniformly distributed, they are uniformly distributed on the simulation region all the time.

In summary, we have showed that this SMS model *unifies* the desired features of mobility models such as smooth movements, stable speed via analysis and simulations, and uniform nodal distribution. To further demonstrate the merits of the proposed model, in the next section, we will discuss how to implement and adapt the SMS model to networking environments. Also, we will illustrate the impacts of the proposed model on link lifetime, and network topology.

6 Implementation and impacts of SMS model

Since the SMS model describes the individual node mobility according to time steps, it can be *flexibly controlled* to simulate diverse moving behaviors including straight lines or curves; short or long trips; stable or

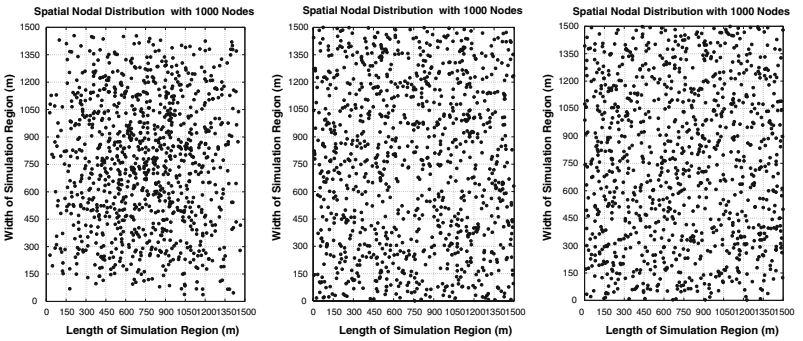

(a) RWP Model at the 1000^{th} sec. **(b)** SMS Model at the 500^{th} sec. **(c)** SMS Model at the1000^{th} sec.

Fig. 8 Top-view of node distribution of RWP model and SMS model

variable speeds; fast or slow speed acceleration and deceleration. Hence, the SMS model can be implemented network simulations requiring flexible control of mobile nodes, for example, the guidance of mobile robots with smooth motion for disaster survivor detection [44] and for navigation across a sensor network [45], or the guidance of mobile agents for better connectivity in MANETs [46]. We will explain the implementation of group mobility and under geographical constraints, followed by the effects of this model on relative speed, link lifetime, and node degree.

The implementation of SMS model is not complex even though the analysis of this model involves time steps at microscopic level and movements at macroscopic level. The key to a successful simulation is to specify *target speed* for α-phase, the time steps for each phase, which determines the granularity of speed change, pause time after a stop, and correlation factor. For the purpose of case studies and applications, we will discuss how to apply the proposed model in different scenarios.

6.1 Extensions to group mobility

Several group mobility models are described in [12, 13, 47] according to different MANET applications. Among these models, *Reference Point Group Mobility* (RPGM) model is the most widely used model; however, the similar problems of abrupt moving behaviors and the average speed decay also exist in RPGM model [47], since the leader in RPGM model moves according to the RWP mobility pattern. Moreover, it is difficult to generate mobility scenarios with different levels of spatial dependency between group members and their leader [12].

Here, we study the extension of SMS model to group mobility for eliminating above limitations in RPGM model. In SMS mobility model, we consider each group with one leader and several group members. Initially, the leader lies in the center of the group, and other group members are uniformly distributed within the geographic scope of the group. The size of the group is dependent on the effective transmission range of the wireless devices and the node density. The group leader dominates the moving behaviors of the entire group, including the node speed, direction and moving duration. Specifically, the velocity of group member m at its nth step is represented as:

$$\begin{cases} V_n^m = V_n^{Leader} + (1-\rho)\cdot U \cdot \Delta V_{\max} \\ \phi_n^m = \phi_n^{Leader} + (1-\rho)\cdot U \cdot \Delta \phi_{\max}, \end{cases} \tag{40}$$

where U is a random variable with uniform distribution over [–1, 1]. $\Delta V_{\max}$ and $\Delta\phi_{\max}$ are the maximum speed and direction difference between a group member and the leader in one time step. $\rho \in [0, 1]$ is the spatial correlation parameter. When ρ approaches to 1, i.e., the spatial correlation between a group member and the leader becomes stronger, the deviation of the velocity of a group member from that of the leader is getting smaller. Therefore, by adjusting the parameter ρ, different SMS group mobility scenarios can be generated.

In SMS group mobility model, the group leader follows the exact mobility patterns defined in the SMS model. The detailed moving behaviors of group members in SMS model are described as follows. At the beginning of an SMS movement, the group leader first selects the target speed ${v_\alpha}^{Leader}$, target direction ${\phi_\alpha}^{Leader}$, and phase period α which is the same as all group members. Then, corresponding to ${v_\alpha}^{Leader}$ and ${\phi_\alpha}^{Leader}$, the target speed ${v_\alpha}^m$ and target direction ${\phi_\alpha}^m$ of group member m are selected from (40). For each time step in β-phase, the speed and direction of a group member are also obtained from (40) according to the reference velocity of the leader at that time step. When the leader transits into γ-phase, similarly, each group member selects its own values of ${v_\beta}^m$ and ${\phi_\gamma}^m$ towards a stop. Thus, the entire group will stop after γ steps. By this means, every group member can evenly accelerate/decelerate the speed in α/γ-phase while keeping the similar

mobility trajectory to the leader. Figure 9 gives an illustration of five nodes traveling within one SMS movement period in the proposed SMS group mobility model with correlation parameter $\rho = 0.9$, where $\Delta V_{\max} = 5$ m/s, and $\Delta\phi_{\max} = \pi/3$. It is observed that all trajectories of group members are in close proximity to that of the leader, as their spatial correlation are strong. Based on the above demonstration, we conclude that SMS model can be easily adapted to group mobility.

6.2 Adaption to geographical constraints

In real world, the movement of nodes are often under geographical constraints such as streets in a city or pathways of obstacles [12, 13]. To achieve a more realistic movement trajectory, Jardosh et al. [48] proposed an *obstacle mobility* model, under the incorporation of randomly selected obstacles, to restrict both node movement as well as wireless transmissions. Also, Bai et al. discussed a *Manhattan* mobility model in [1].

We observed that the typical moving behaviors of vehicles match the four-phase mobility pattern in the SMS model very well. Besides, vehicular ad hoc networking (VANET) designed for safety driving and commercial applications is a very important research branch of MANETs. As an example, we discuss how to use SMS model with geographical extension to simulate moving behaviors of vehicles in a Manhattan-like city map. Figure 10 illustrates the map applied for our SMS model.

As shown in Fig. 10, each line segment represents a bi-directional street of the city. The speed limit associated with each type of street is labeled on the right side of the map. In this model, the coordinate of intersection points between streets and the street speed limit are known for all nodes. Initially, mobile nodes are randomly deployed in the streets. Each mobile node randomly chooses a destination

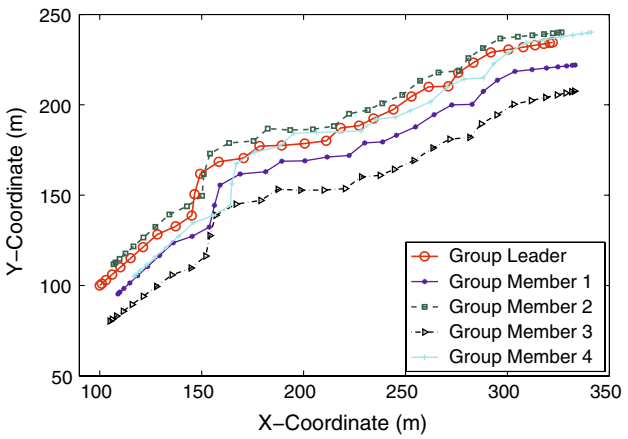

Fig. 9 Group mobility with SMS model

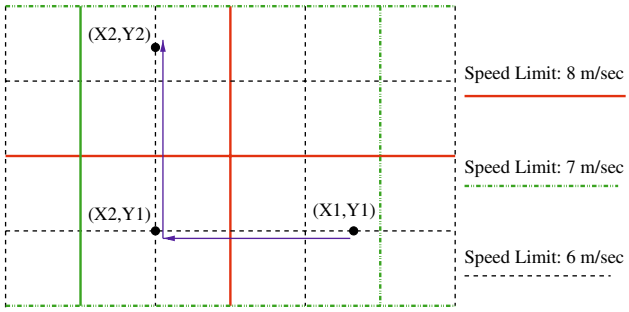

Fig. 10 Use SMS model in a Manhattan-like area

and finds the shortest path using Dijkstra's algorithm for the next movement. For example, in Fig. 10, the node located in (X_1, Y_1) will reach the destination (X_2, Y_2) through the intersection point (X_2, Y_1). Because mobile nodes are only allowed to move along the predefined pathways in the map, the adapted SMS model describes a straight line movement without direction change for each trip. Thus, the moving behavior of an SMS node along the street is pseudo-random. For each straight line movement, the moving behaviors of the SMS node comply the following rules:

$$\sqrt{(X_i - X_j)^2 + (Y_i - Y_j)^2} = \frac{V}{2}\alpha + V\beta + \frac{V}{2}\gamma, \tag{41}$$

where V is the target speed and will not change during the β-phase. The selection of V is determined by the associated street speed limit V_{limit}, such that $V \in [V_{limit} - \epsilon, V_{limit}]$, where ε is a small positive value. In this way, the SMS movement along the street is a typical movement with even speed acceleration and deceleration without speed decay problem. Moreover, the SMS node can properly stop at the target intersection point, such as (X_2, Y_1) in this example.

6.3 Effects of SMS model

Almost all mobility models used in current simulation tools, such as RWP model utilized in ns-2, describe completely uncorrelated mobility. The abrupt speed and direction change events, induced by these models, will influence the network topology change rate, which further significantly affects the routing performance of the network. Therefore, the simulation results and theoretical derivations, based on current mobility models in the simulation tools, may not correctly indicate the real-life network performance and effects of system parameters. Since the SMS model provides more realistic moving behaviors than current random mobility models, we apply the model to estimate the network performance based on connectivity metrics. Meanwhile, we want to find out whether the evaluation results are much different from random mobility

models, for example the RWP model; and how different they are.

To generate different mobility levels for both RWP and SMS models, we respectively set the initial average speed $E\{v_{ini}\}$ as 2, and 15 m/s. The PDFs of the relative speed of two models according to the different initial average speed $E\{v_{ini}\}$ are shown in Fig. 11. For a pair of neighboring nodes (u, w), the relative speed $\overrightarrow{V^u}$ of node u according to the reference node w consists of two components in terms of X-axis and Y-axis of a Cartesian coordinate system centered at node w. Specifically, in the smooth model, the magnitude of nth step relative speed of node u is: $|V_n^u| = \sqrt{(X_n - X_{n-1})^2 + (Y_n - Y_{n-1})^2}$, where X_{n-1}/X_n is the starting/ending coordinate of the nth step relative trip of node u in X-axis, so is Y_{n-1}/Y_n for Y-axis. Since $\Delta t = 1$ s, $n \gg 1$. Based on the central limit theorem (CLT) [34], when $n \gg 1$, both i.i.d random variable $X_n - X_{n-1}$ and $Y_n - Y_{n-1}$ can be effectively approximated by an identical Gaussian distribution with zero mean [49]. Furthermore, for any two independent Gaussian RVs, for example A and B, with zero mean and equal variance, the RV $Z = \sqrt{A^2 + B^2}$ has a *Rayleigh density*. Hence, the relative speed V_n^u in the smooth model has an approximate Rayleigh distribution, which exactly matches the results shown in Fig. 11 of both scenarios with different $E\{v_{ini}\}$. However, because of the speed decay [17] and abrupt velocity change problems [12], the PDF of relative speed in the RWP model varies irregularly during the simulation and tends to have larger proportion in the region of small speed. This phenomenon shows more apparently when $E\{v_{ini}\}$ is large.

As the relative speed has a significant effect on the link lifetime, we further evaluate the CDF of link lifetime between these two models. Here, we specify $E\{v_{ini}\}$ as 2 m/s. To investigate the effect of temporal correlation of node velocity in β-phase on link lifetime, we respectively set the memorial parameter ζ as 0, 0.5, and 1 in the SMS model. The simulation results are shown in Fig. 11(b). Given (3), when $\zeta = 1$, the node velocity has the strongest correlation, and the entire movement is a straight line according to the direction ϕ_α. In contrast, when $\zeta \neq 1$, the successive direction change in the β-phase increases the chance of link failures. Thus, from Fig. 11(b), in the region of short link lifetime, the corresponding CDF for $\zeta = 1$ is evidently less than that for $\zeta = 0$ and $\zeta = 0.5$. Based on (28), the SMS model generates stable average speed according to $E\{v_{ini}\}$, regardless of the value of ζ. Given $E\{v_{ini}\} = 2$ m/s, we find that the expected link lifetime of the SMS model based on different ζ is almost same and around 100 s. In contrast, for the RWP model, because of the speed decay problem, the relative speed between RWP nodes is generally less than that in SMS model. Hence, the lower mobility level and lower topology change rate increase the link lifetime in the RWP model. From Fig. 11(b), we can see that the uptrend of CDF of link lifetime for the RWP model is dramatically less than that for the SMS model. Meanwhile, the expected link lifetime of the RWP model is 168 s, which is much longer than that of the SMS model. Therefore, according to Fig. 11(b), we find that the link lifetime analysis and evaluation in MANETs via macroscopic random mobility models, such as RWP model, may invalidate and even lead to wrong conclusions.

Due to different spatial node distributions, mobility models with same node density (σ) would yield different average node degree during the simulation. As the default transmission range $R = 250$ m for mobile nodes in ns-2, in a square area of size 1401 m^2, the node density of each model is $\sigma = 5/(\pi R^2)$. Thus, on average each node would have four neighbors during the simulation. Figure 11(c) illustrates the percentage of nodes whose node degree is no less than four during the simulation between these two models. We find that the result obtained in the RWP model is apparently larger than that of smooth model. This is because the majority of nodes move into the center region in the RWP model as time goes by [18]. In consequence, because of the longer average link lifetime and higher network connectivity, the ad hoc routing protocol performance based on RWP model with regards to average hop count, end-to-end network throughput, end-to-end packet delay and routing overhead is "better" than that of the SMS model. Therefore, we conclude that the network connectivity and routing protocols evaluation based

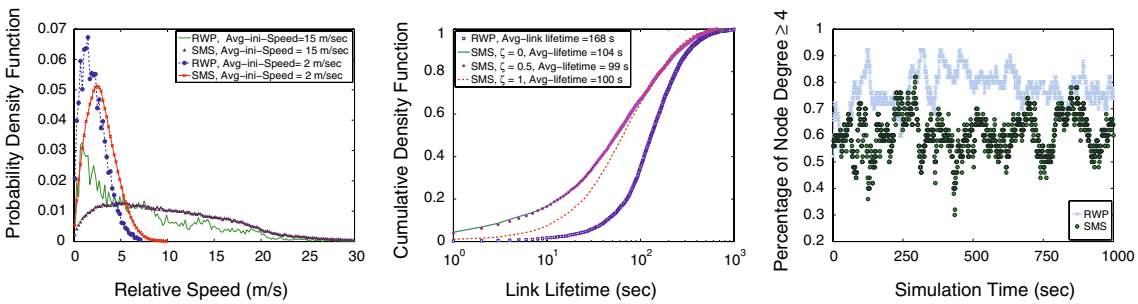

(a) PDF of Relative Speed. **(b)** CDF of Link Life time. **(c)** Node Degree.

Fig. 11 Network connectivity performance comparison between the RWP and the SMS model

on RWP model could be over optimistic. Thus, the SMS model, which generates stable speeds and maintains uniform node distribution, is more preferable for network connectivity study and routing protocols evaluation in MANETs.

7 Conclusions

In this article, we proposed a novel mobility model, *Semi-Markov Smooth* (SMS) model which can *unify* the desired features of a mobility model. The mobility pattern defined in the SMS model has memorial property between successive step trips and is consistent with the physical law of motion in real environments. Based on the stochastic analysis, we proved that there is no average speed decay in the SMS model regardless of initial speed and the SMS model maintains uniform node distribution during the entire simulation period. These properties are also validated by simulations. We also demonstrated that the SMS model can be extended to group mobility and adapted to geographical constraints. Moreover, we evaluate the application effects of SMS model with respect to the PDF of relative speed between a pair of neighboring nodes, the CDF of link lifetime, and node degree in MANETs. Because the SMS model possesses a variety of nice properties and it satisfies the requirements of a "sound mobility model" introduced in [25], this model can be used as a benchmark mobility model for evaluating the performance of various mobile wireless networks.

Appendix

Derivation of the PMF of movement steps $\mathcal{K}$

Let $\mathcal{K} = \mathcal{Z} + \gamma$, where $\mathcal{Z} = \alpha + \beta$. Then, we derive the pmf of $\mathcal{K}$ by two steps. First, we derive the pmf of random variable $\mathcal{Z}$, which is the function (summation) of two independent uniform discrete random variables. The similar example for deriving the pdf of summation two independent continuous random variables is shown in Sect. 6-2 in [34]. By substituting $\alpha_{\min}$, $\beta_{\min}$ and $\alpha_{\max}$, $\beta_{\max}$ with N_{min} and N_{max}, respectively, the pmf of $\mathcal{Z}$ is derived as:

$$Prob\{\mathcal{Z} = Z\} = \begin{cases} \frac{Z-2N_{min}+1}{(N_{max}-N_{min}+1)^2} & 2N_{min} \le Z \le N_{min}+N_{max} \\ \frac{2N_{max}+1-Z}{(N_{max}-N_{min}+1)^2} & N_{min}+N_{max} \le Z \le 2N_{max} \end{cases} \tag{42}$$

Second, we obtain the pmf of $\mathcal{K}$ which is summation of random variable $\mathcal{Z}$ and uniform random variable γ. Figure 12 illustrates a rectangular region inside the $\gamma - \mathcal{Z}$ coordinates, which is the intersection area of the domains between γ and $\mathcal{Z}$. This rectangular region is split into three zones by two dotted lines. For each zone, the pmf of $\mathcal{K}$ is derived with respect to three disjoint intervals of domain $\mathcal{K}$. For zone 1, where $3N_{min} \le k \le 2N_{min} + N_{max}$.

$$\begin{aligned} &Prob\{\mathcal{K} = k\} \\ &= \sum_{r=b}^{k-2N_{min}} P\{\gamma = r\}P\{\mathcal{Z} = k-r\} \\ &= \sum_{r=b}^{k-2N_{min}} \frac{1}{(N_{max}-N_{min}+1)} \frac{k-r-2N_{min}+1}{(N_{max}-N_{min}+1)^2} \\ &= \frac{k^2 - 6k\cdot N_{min} + 3k + 9N_{min}^2 - 9N_{min} + 2}{2(N_{max}-N_{min}+1)^3}. \end{aligned} \tag{43}$$

For zone 2, where $2N_{min} + N_{max} \le k \le N_{min} + 2N_{max}$, by assuming $2N_{min} + N_{max} \le N_{min} + 2N_{max}$.

$$\begin{aligned} &Prob\{\mathcal{K} = k\} \\ &= \sum_{r=N_{min}}^{k-(N_{min}+N_{max})} P\{\gamma = r\}P\{\mathcal{Z} = k-r\} + \sum_{r=k-(N_{min}+N_{max})+1}^{N_{max}} P\{\gamma = r\}P\{\mathcal{Z} = k-r\} \\ &= \frac{1}{(N_{max}-N_{min}+1)^3} \left(\sum_{r=N_{min}}^{k-(N_{min}+N_{max})} (2N_{max}+1-k+r) + \sum_{r=k-(N_{min}+N_{max})+1}^{N_{max}} (k-r-2N_{min}+1) \right) \\ &= \frac{6k(N_{min}+N_{max}) - 2k^2 - 3(N_{min}^2 + N_{max}^2 + 4N_{min}\cdot N_{max} + N_{min} - N_{max}) + 2}{2(N_{max}-N_{min}+1)^3}. \end{aligned} \tag{44}$$

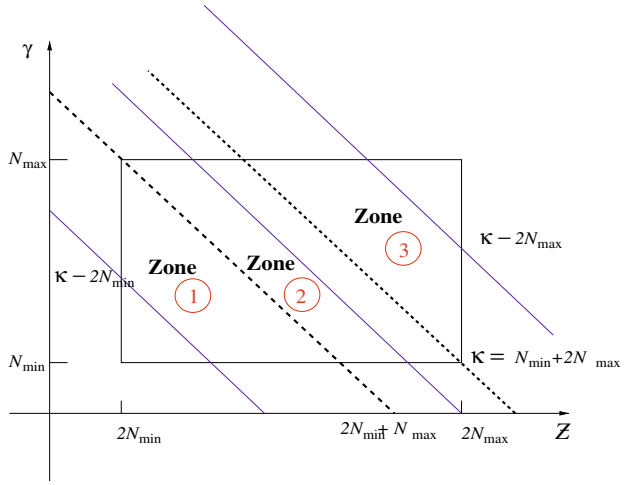

Fig. 12 Different domain intervals of $\mathcal{K}$

For zone 3, where $2N_{max} + N_{min} \le k \le 3N_{max}$.

$$\begin{aligned} &Prob\{\mathcal{K}=k\} \\ &=\sum_{r=k-2N_{max}}^{N_{max}} P\{\gamma=r\}P\{\mathcal{Z}=k-r\} \\ &=\sum_{r=k-2N_{max}}^{N_{max}} \frac{1}{(N_{max}-N_{min}+1)}\frac{2N_{max}+1-k+r}{(N_{max}-N_{min}+1)^2} \\ &=\frac{k^2-6k\cdot N_{max}-3k+9N_{max}^2+9N_{max}+2}{2(N_{max}-N_{min}+1)^3}. \end{aligned} \tag{45}$$

By combining (43)–(45), we can obtain the complete pmf of $\mathcal{K}$ shown in (8).

Derivation of the CDF of steady state speed v_{ss}

The cumulative density function (CDF) of steady state speed v_{ss} can be derived from the limiting fraction of time when step speeds are less than v, as the simulation time t approaches to infinity. When $t \to \infty$, $N(t) \to \infty$, we have

$$\begin{aligned} &Pr\{v_{ss}\le v\} \\ &=\lim_{t\to\infty}\frac{\sum_{n=1}^{\mathcal{M}(t)}\mathbf{1}_{\{v_n\le v\}}+\sum_{n=1}^{\mathcal{M}_p(t)}\mathbf{1}_{\{v_n\le v\}}}{\mathcal{M}(t)+\mathcal{M}_p(t)}=\lim_{N(t)\to\infty}\frac{\sum_{i=1}^{N(t)}\sum_{j=1}^{T(i)}\mathbf{1}_{\{v(i,j)\le v\}}+T_p(i)}{\sum_{i=1}^{N(t)}(T(i)+T_p(i))} \\ &=\lim_{N(t)\to\infty}\frac{\frac{1}{N(t)}\sum_{i=1}^{N(t)}}{\frac{1}{N(t)}\sum_{i=1}^{N(t)}(T(i)+T_p(i))}\left(\sum_{j=1}^{\alpha(i)}\mathbf{1}_{\{v(i,j)\le v\}}+\sum_{j=\alpha(i)+1}^{\alpha(i)+\beta(i)}\mathbf{1}_{\{v(i,j)\le v\}}+\sum_{j=\alpha(i)+\beta(i)+1}^{T(i)}\mathbf{1}_{\{v(i,j)\le v\}}+T_p(i)\right). \end{aligned} \tag{46}$$

Let $R_i(v)$ denote the total time when step speeds are less than v in the ith movement. From (46), $R_i(v)$ represents as:

$$\begin{aligned} R_i(v)=&\sum_{j=1}^{\alpha(i)}\mathbf{1}_{\{v(i,j)\le v\}}+\sum_{j=\alpha(i)+1}^{\alpha(i)+\beta(i)}\mathbf{1}_{\{v(i,j)\le v\}} \\ &+\sum_{j=\alpha(i)+\beta(i)+1}^{T(i)}\mathbf{1}_{\{v(i,j)\le v\}}. \end{aligned} \tag{47}$$

In a discrete-time SMS process, $\{R(v)\}_i$, $\{T\}_i$, and $\{T_p\}_i$ are all i.i.d. random sequences, i.e., $E\{T(i)\} = E\{T\}$, $E\{T_p(i)\} = E\{T_p\}$, and $E\{R(v)_i\} = E\{R(v)\}$. As $N(t) \to \infty$, by the strong law of large number, from (46) and (47), $Pr\{v_{ss} \le v\}$ is derived as:

$$\begin{aligned} Pr\{v_{ss}\le v\}=&\frac{1}{E\{T\}+E\{T_p\}}\cdot\left(E\{T_p\}+E\left\{\sum_{j=1}^{\alpha}\mathbf{1}_{\{v_j\le v\}}\right.\right. \\ &\left.\left.+\sum_{j=\alpha+1}^{\alpha+\beta}\mathbf{1}_{\{v_j\le v\}}+\sum_{j=\alpha+\beta+1}^{T}\mathbf{1}_{\{v_j\le v\}}\right\}\right) \\ =&\frac{E\{R(v)\}+E\{T_p\}}{E\{T\}+E\{T_p\}}. \end{aligned} \tag{48}$$

Based on (48), we derived $E\{R(v)\}$ with respect to α-phase, β-phase, and γ-phase as follows.

1. The average total time when step speeds in α-phase of one movement are lower than v is:

$$\begin{aligned} E\left\{\sum_{j=1}^{\alpha}\mathbf{1}_{\{v_j\le v\}}\right\}&=\sum_{m=N_{min}}^{N_{max}}\sum_{j=1}^{\alpha}E\{\mathbf{1}_{\{v_\alpha(j)\le v\}}\}E\{\mathbf{1}_{\{\alpha=m\}}\} \\ &=\sum_{m=N_{min}}^{N_{max}}\sum_{j=1}^{m}Pr\{\alpha=m\}Pr\left\{\frac{v_\alpha}{m}j\le v\right\} \\ &=\frac{1}{N_{max}-N_{min}+1}\sum_{m=N_{min}}^{N_{max}}\sum_{j=1}^{m}\int_{v_{\min}}^{\frac{v\cdot m}{j}}f_{v_\alpha}(v)dv. \end{aligned} \tag{49}$$

2. The average total time when step speeds in β-phase of one movement are lower than v is:

$$E\left\{\sum_{j=\alpha+1}^{\alpha+\beta}\mathbf{1}_{\{v_j\le v\}}\right\}=\sum_{m=N_{min}}^{N_{max}}\sum_{j=1}^{\beta}E\{\mathbf{1}_{\{v_\beta(j)\le v\}}\}E\{\mathbf{1}_{\{\beta=m\}}\}$$
$$=\sum_{m=N_{min}}^{N_{max}}\sum_{j=1}^{m}Pr\{\beta=m\}Pr\{v_\beta(j)\le v\}$$
$$=\frac{1}{N_{max}-N_{min}+1}\sum_{m=N_{min}}^{N_{max}}\sum_{j=1}^{m}\int_0^v f_{v_\beta(j)}(v)dv. \tag{50}$$

3. The average total time when step speeds in γ-phase of one movement are lower than v is:

$$E\left\{\sum_{j=\alpha+\beta+1}^{T}\mathbf{1}_{\{v_j\le v\}}\right\}$$
$$=\sum_{m=N_{min}}^{N_{max}}\sum_{j=1}^{\gamma}E\{\mathbf{1}_{\{v_\gamma(j)\le v\}}\}E\{\mathbf{1}_{\{\gamma=m\}}\}$$
$$=\sum_{m=N_{min}}^{N_{max}}\sum_{j=1}^{m}Pr\{\gamma=m\}Pr\left\{v_\beta\left(1-\frac{j}{m}\right)\le v\right\} \tag{51}$$
$$=\frac{1}{N_{max}-N_{min}+1}\sum_{m=N_{min}}^{N_{max}}\sum_{j=1}^{m}\int_0^{\frac{v\cdot m}{m-j}}f_{v_\beta}(v)dv.$$

By combining (48) to (51), we obtain the value of $E\{\ R(v)\}$ and show the final CDF result of v_{ss} in (27).

Derivation of expected steady state speed $E\{v_{ss}\}$

Based on (30), We derive four components of $E\{v_{ss}\}$ according to each state of embedded semi-Markov chain $\{\mathcal{Y}_n\}$ as follows.

1. The average steady state speed $E_\alpha\{v_{ss}\}$ in α-phase is:

$$E_\alpha\{v_{ss}\}=\frac{\sum_{m=N_{min}}^{N_{max}}\sum_{j=1}^{m}Pr\{\alpha=m\}\int_v v\cdot\frac{m}{j}f_{v_\alpha}(\frac{v\cdot m}{j})dv}{E\{T\}+E\{T_p\}}$$
$$=\frac{\sum_{m=N_{min}}^{N_{max}}Pr\{\alpha=m\}\sum_{j=1}^{m}\frac{j}{m}\cdot E\{v_\alpha\}}{E\{T\}+E\{T_p\}}$$
$$=\frac{E\{v_\alpha\}\sum_{m=N_{min}}^{N_{max}}\frac{1+m}{2}Pr\{\alpha=m\}}{E\{T\}+E\{T_p\}}$$
$$=\frac{\frac{1}{2}E\{v_\alpha\}(1+E\{\alpha\})}{E\{T\}+E\{T_p\}}. \tag{52}$$

2. The average steady state speed $E_\beta\{v_{ss}\}$ in β-phase is:

$$E_\beta\{v_{ss}\}=\frac{\sum_{m=N_{min}}^{N_{max}}\sum_{j=1}^{m}Pr\{\beta=m\}E\{v_\beta(j)\}}{E\{T\}+E\{T_p\}}$$
$$=\frac{E\{v_\alpha\}\sum_{m=N_{min}}^{N_{max}}mPr\{\beta=m\}}{E\{T\}+E\{T_p\}} \tag{53}$$
$$=\frac{E\{v_\alpha\}E\{\beta\}}{E\{T\}+E\{T_p\}}.$$

3. The average steady state speed $E_\gamma\{v_{ss}\}$ in γ-phase is:

$$E_\gamma\{v_{ss}\}=\frac{\sum_{m=N_{min}}^{N_{max}}\sum_{j=1}^{m}Pr\{\gamma=m\}\int_v v\cdot\frac{m}{m-j}f_{v_\beta}(\frac{v\cdot m}{m-j})dv}{E\{T\}+E\{T_p\}}$$
$$=\frac{\sum_{m=N_{min}}^{N_{max}}Pr\{\gamma=m\}\sum_{j=1}^{m}\frac{m-j}{m}\cdot E\{v_\beta\}}{E\{T\}+E\{T_p\}}$$
$$=\frac{E\{v_\alpha\}\sum_{m=N_{min}}^{N_{max}}\frac{1}{m}Pr\{\gamma=m\}\sum_{j=0}^{m-1}j}{E\{T\}+E\{T_p\}}$$
$$=\frac{E\{v_\alpha\}\sum_{m=N_{min}}^{N_{max}}\frac{m-1}{2}Pr\{\gamma=m\}}{E\{T\}+E\{T_p\}}$$
$$=\frac{\frac{1}{2}E\{v_\alpha\}(E\{\gamma\}-1)}{E\{T\}+E\{T_p\}}. \tag{54}$$

4. The average steady state speed $E_{I_p}\{v_{ss}\}$ in pause phase is:

$$E_{I_p}\{v_{ss}\}=\int_v v\cdot\frac{E\{T_p\}\delta(v)}{E\{T\}+E\{T_p\}}dv=0. \tag{55}$$

By combining (52) to (55), we obtain the expected steady state speed $E\{v_{ss}\}$, which is shown in (32).

References

1. Bai, F., Sadagopan, N., Krishnamachari, B., & Helmy, A. (2003). "Important: A framework to systematically an-alyze the impact of mobility on performance of routing protocols for ad hoc networks," in *Proc. of IEEE INFOCOM*, Vol. 2, San Francisco, CA, USA, 825–835
2. Sadagopan, N., Bai, F., Krishnamachari, B., & Helmy, A. (2003). "Paths: Analysis of path duration statistics and their impact on reactive manet routing protocols," in *Proc. of ACM MobiHoc*, Annapolis, MD, USA, 245–256
3. Jain, R., Lelescu, D., & Balakrishnan, M. (2005). "Model T: An empirical model for user registration patterns in a campus wireless LAN," in *Proc. of ACM MobiCom*, Cologne, Germany, 170–184
4. Kyriakakos, M., Frangiadakis, N., Merakos, L., & Hadjiefthymiades, S. (2003). "Enhanced path prediction for network resource management in wireless LANs", *IEEE Wireless Communications, Vol. 10*, 62–69
5. Iraqi, Y., Ghaderi, M., & Boutaba, R. (2004). "Enabling real-time All-IP wireless networks," in *Proc. of IEEE Wireless Communications and Networking Conference (WCNC)*, Vol. 3, Atlanta, Georgia, USA, 1500–1505

6. Gupta, V., & Dixit, A. (1996). "The design and deployment of a mobility supporting network," in *Proc. of international Symposium on Parallel Architectures, Algorithms, and Networks, 1996*., Beijing, China, 228–234, IEEE Computer Society
7. Cheng, M., Cardei, M., Sun, J., Cheng, X., Wang, L., Xu. Y., & Du, D. -Z. (2004). "Topology control of ad hoc wireless networks for energy efficiency", *IEEE Transactions on Computers, Vol. 53*, 1629–1635
8. Borkar, V., & Manjunath, D. (2005). "Distributed topology control of wireless networks," in *Proc. of 3rd IEEE International Symposium on Modeling and Optimization in Mobile, Ad Hoc and Wireless Networks (WIOPT)*, Garda, Trentino, Italy, 155–163
9. Grossglauser, M., & Tse, D. (2001). "Increases the capacity of ad-hoc wireless networks," in *Proc. of IEEE INFO-COM*, Vol. 3, Anchorage, Alaska, USA, 1360–1369
10. Bettstetter, C. (2004). "On the connectivity of ad hoc networks," *Computer Journal, Special Issue on Mobile and Pervasive Computing, 4*, 432–447
11. Yuen, W.H., & Sung, C.W. (2003). "On energy efficiency and network connectivity of mobile ad hoc networks," in *Proc. of 23rd IEEE International Conference on Distributed Computing Systems*, Providence, RI, USA, 38–45
12. Bettstetter, C. (2001). "Smooth is better than sharp: A random mobility model for simulation of wireless networks," in *Proc. of ACM International Symposium on MSWiM*. (Rome, Italy) 19–27
13. Camp, T., Boleng, J., & Davies, V. (2002). "A survey of mobility models for ad hoc networks research," *Wireless Communication and Mobile Computing (WCMC): Special issue on Mobile Ad Hoc Networking: Research, Trends and Applications*, *Vol. 2 (5)*, 483–502
14. Song, L., Kotz, D., Jain, R., & He, X. (2004). "Evaluating location predictors with extensive Wi-Fi mobility data," in *Proc. of IEEE INFOCOM*, Vol. 2, Hong Kong, China, 1414–1424
15. Chinchilla, F., Lindsey, M., & Papadopouli, M. (2004). "Analysis of Wireless information locality and association patterns in a campus," in *Proc. of IEEE INFOCOM*, Vol. 2, Hong Kong, China, 906–917
16. Johnson, D.B., & Maltz, D.A. (1996). "Dynamic source routing in ad hoc wireless networks," in *Mobile Computing* (Imielinski and Korth, eds.), Vol. 353, Ch. 5, 153–181, Kluwer Academic Publishers
17. Yoon, J., Liu, M., & Noble, B. (2003). "Random waypoint considered harmful," in *Proc. of IEEE INFOCOM*, Vol. 2, San Francisco, CA, USA, 1312–1321
18. Bettstetter, C., Resta, G., & Santi, P. (2003). "The node distribution of the random waypoint mobility model for wireless ad hoc networks," *IEEE Transactions on Mobile Computing*, *Vol. 2*, 257–269
19. Blough, D. M., Resta, G., & Santi, P. (2004). "A Statistical analysis of the long-run node spatial distribution in mobile ad hoc networks," *ACM Wireless Networks*, *Vol. 10*, 543–554
20. Royer, E., Melliar-Smith, P., & Moser, L. (2001). "An analysis of the optimum node density for ad hoc mobile networks," in *Proc. of IEEE International Conference on Communications (ICC)*, Vol. 3, Helsinki, Finland, 857–861
21. Nain, P., Towsley, D., Liu, B., & Liu, Z. (2005). "Properties of random direction models," in *Proc. of IEEE INFOCOM*, Vol. 3, Miami, FL, USA, 1897–1907
22. Boudec, J.-Y.L., & Vojnovic, M. (2005). "Perfect simulation and stationarity of a class of mobility models," in *Proc. of IEEE INFOCOM*, Vol. 4, Miami, FL, USA, 2743–2754
23. Liang, B., & Haas, Z. (1999). "Predictive distance-based mobility management for pcs networks," in *Proc. of IEEE INFOCOM*, Vol. 3, (New York, NY, USA), 1377–1384
24. Zhao, M., & Wang, W. (2006). "A Novel Semi-Markov Smooth Mobility Model for Mobile Ad Hoc Networks," in *Proc. of IEEE GLOBECOM*, **Best Student Paper Award**-*Communication Networks*
25. Yoon, J., Liu, M., & Noble, B. (2003). "Sound mobility models," in *Proc. of ACM MobiCom*, San Francisco, CA, USA, 205–216
26. Fang, Y., Chlamtac, I., & Lin, Y. -B. (2000). "Portable movement modeling for PCS networks," *IEEE Transactions on Vehicular Technology, Vol. 46*, 1356–1363
27. Wang, G., Cao, G., & Porta, T.L. (2004). "Movement-assisted sensor deployment," in *Proc. of IEEE INFOCOM*, Vol. 4, Hong Kong, China, 2469–2479
28. Bansal, N., & Liu, Z. (2003). "Capacity, delay and mobility an wireless ad-hoc networks," in *Proc. of IEEE INFOCOM*, San Francisco, CA, USA, 1553–1563
29. Samar, P., & Wicker, S.B. (2004). "On the behavior of communication links of node in a multi-hop mobile environment," in *Proc. of ACM MobiHoc*, Tokyo, Japan, 145–156
30. McGuire, M. (2005). "Stationary distribution of random walk mobility models for wireless ad hoc networks," in *Proc. of ACM MobiHoc*, Urbana-Champaign, IL, USA, 90–98
31. Feller, W. (1971). *An Introduction to Probability Theory and Its Applications, Volume II*. Wiley Series in Probability and Mathematical Statistics, 2 ed.
32. Heyman, D.P., & Sobel, M.J. (1982). *Stochastic Models in Operations Research, Volume I*. McGraw-Hill, 2 ed.
33. Shiryaev, A. (1995) *Probability*. Springer, 2 ed.
34. Papoulis, A. (1991). *Probability, Random Variables, and Stochastic Process*. McGraw-Hill
35. Camp, T., Boleng, J., Williams, B., Wilcox, L., & Navidi, W. (2002). "Performance comparison of two location based routing protocols for ad hoc networks," in *Proc. of IEEE INFOCOM*, New York, NY, USA, 1678–1687
36. Ko, Y.-B., & Vaidya, N.H. (1998). "Location-aided routing (LAR) in mobile ad hoc networks," in *Proc. of ACM MobiCom*, Dallas, Texas, USA, 66–75
37. Boleng, J., & Camp, T. (2003). "Adaptive location aided mobile ad hoc network routing," Technical Report MCS-03-09, The Colorado School of Mines
38. Li, J., & Mohapatra, P. (2003). "Laker: Location aided knowledge extraction routing for mobile ad hoc networks," in *Proc. IEEE WCNC*, Vol. 2, New Orleans, LA, USA, 1180–1184
39. Li, J., Jannotti, J., DeCouto, D., Krager, D., & Morris, R. (2000). "A scalable location service for geographic ad-hoc routing," in *Proc. of ACM Mobicom*, Boston, MA, USA, 120–130
40. "Psi function. http://mathworld.Wolfram.com/digammafunction.html"
41. "The network simulator ns-2. http://www.isi.edu/nsnam/ns/,"2003
42. Lin, G., Noubir, G., & Rajaraman, R. (2004). "Mobility models for ad hoc network simulation," in *Proc. of IEEE INFOCOM*, Vol. 1, Hong Kong, China. 454–463
43. Navidi, W., & Camp, T. (2004). "Stationary distributions for the random way point mobility model," *IEEE Transactions on Mobile Computing, Vol. 3*, 99–108
44. Aoyama, H., Himoto, A., Fuchiwaki, O., Misaki, D., & Sumrall, T. (2005). "Micro hopping robot with IR sensor for disaster survivor detection,"in *Proc. of IEEE International workshop on Safety, Security and Rescue Robotics*, kobe, Japan, 189–194
45. Li, Q., Rosa, M.D., & Rus, D. (2003). "Distributed algorithms for guiding navigation across a sensor network," in *Proc. of ACM Mobicom*, San Francisco, CA, USA, 313–325
46. Agarwal, P. K., Guibas, L. J., & etal., H. E. (2002). "Algorithmic issues in modeling motion," *ACM Computing Surveys (CSUR), Vol. 34* (4), 550–572
47. Hong, X., Gerla, M., Pei, G., & Chiang, C. (1999). "A group mobility model for ad hoc wireless networks," in *Proc. of ACM International Symposium on MSWiM*, Seattle, Washington, USA, 53–60

48. Jardosh, A., Belding-Royer, E. M., Almeroth, K. C., & Suri, S. (2003). "Towards realistic mobility models for mobile ad hoc networks," in *Proc. of ACM Mobicom*, San Francisco, CA, USA, 217–229
49. McDonald, A. B., & Znati, T. F. (1999). "A mobility-based framework for adaptive clustering in wireless ad hoc networks," *IEEE Journal on Selected Areas in Communications, Vol. 17*, 1466–1487

Author Biographies

Ming Zhao received the B.S. of Electrical Engineering from Harbin Institute of Technology in 1997. He received the M.S.E.E. from China Academy of Telecommunications Technology in 2000 and New York State University at Buffalo in 2004, respectively. He is currently a Ph.D. student with the Department of Electrical and Computer Engineering, North Carolina State University. His current research interest include mobility modeling, network topology, and mobility management in wireless networks.

Wenye Wang (M'98/ ACM'99) received the B.S. and M.S. degrees from Beijing University of Posts and Telecommunications, Beijing, China, in 1986 and 1991, respectively. She also received the M.S.E.E. and Ph.D. degree from Georgia Institute of Technology, Atlanta, Georgia in 1999 and 2002, respectively. She is now an Assistant Professor with the Department of Electrical and Computer Engineering, North Carolina State University. Her research interests are in mobile and secure computing, quality-of-service (QoS) sensitive networking protocols in single- and multi-hop networks. She has served on program committees for IEEE INFOCOM, ICC, ICCCN in 2004. Dr. Wang is a recipient of NSF CAREER Award in 2006. She has been a member of the Association for Computing Machinery since 2002.